

**Assessing marine mammal presence in and near the FORCE Lease Area during winter and early spring – addressing baseline data gaps and sensor performance**

Submitted by  
Dr Anna Redden and Peter Porskamp  
Acadia University

to the

Offshore Energy Research Association (OERA)  
and  
Fundy Ocean Research Center for Energy (FORCE)

**FINAL REPORT - 2015**

**Citation:**

Porskamp, P., A.M. Redden, J.E. Broome, B. Sanderson and J. Wood. 2015. Assessing marine mammal presence in and near the FORCE Lease Area during winter and early spring – addressing baseline data gaps and sensor performance. Final Report to the Offshore Energy Research Association and the Fundy Ocean Research Center for Energy. ACER Technical Report No 121, 35 pp, Acadia University, Wolfville, NS, Canada.



## **Assessing marine mammal presence in and near the FORCE Lease Area during winter and early spring – addressing baseline data gaps and sensor performance**

### **Project Summary**

Developments to test TISEC devices and harness tidal energy from high flow sites in the Minas Passage require examination of the potential effects of tidal turbines on the environment, including impacts on marine mammals. Studies conducted to date, at and near the Fundy Ocean Research Centre for Energy (FORCE) in-stream tidal turbine test site in Minas Passage, have included passive acoustic monitoring (PAM) of harbour porpoises during late spring, summer and fall months (Tollit et al., 2011; Wood et al., 2013). This study reports on winter and early spring (Dec-May) baseline data on harbour porpoise presence in Minas Passage during 2013-2014 and addresses both the winter data gap and the performance of different hydrophone technologies deployed in Minas Passage.

We conducted the winter/spring survey of marine mammals at multiple locations in and near the FORCE site during Dec 2013 – June 2014, with the use of C-POD porpoise detectors (Chelonia Ltd) and the icListenHF smart hydrophone (Ocean Sonics Ltd). Both technologies are non-invasive and continuously monitor harbour porpoise click trains within their operational detection range. The main objectives of this study were to close the seasonal (winter/spring) gap in data on harbour porpoise activity in Minas Passage and to determine detection range (distance from hydrophone) and performance in relation to varying tidal conditions for each of the hydrophone technologies examined.

Winter-spring data collected from SUB buoy mounted C-PODS at four of the prior PAM sites showed low presence during winter with activity increasing in March and peaking in June when Atlantic herring and other fishes are known to be present in high abundance. The new data were pooled with all previous C-POD data from the Minas Passage (2010-2012 dataset) prior to data analyses. A new GAM/GEE model was prepared with plots of covariates showing porpoise detection results in relation to Julian Day (seasonal trends), noise (as indicated by C-POD performance metrics - % Time Lost), day vs. night, location, tidal height and current speed. The full dataset (2010-2014) and revised statistical model provide year-round baseline conditions for comparison with studies that will be conducted following turbine installation and operation.

In-field testing of hydrophone performance involved assessing the detection range of each device type (C-POD and icListenHF) housed in a weighted instrument platform resting on the bottom of the FORCE test site. A surface drifting speaker (icTalk, 120-140 kHz) was programmed to transmit at a set rate. All range test C-POD CP1 files and icListenHF spectrograms were visually inspected. C-PODs detected icTalk transmissions up to 300 m from the sound source, with detection efficiency (proportion of transmissions detected; also known as “recall”) greatest within 100 m. Detections, however, were uncommon at depth-averaged current speeds of >1m/s. Data files from a shrouded (20 ppi, ½ inch acoustic foam) icListenHF hydrophone, when visually analyzed by a human, showed icTalk transmission detections at distances up to 300 m (>30% icTalk transmissions detected), with 100% detection efficiency at distances up to 150m.

Harbour porpoise detections recorded by C-PODs housed on the platform were considerably greater than those shown for a co-located C-POD in a SUB buoy moored 2-3 m off the seafloor. Factors that appear to affect performance of SUB buoy mounted C-PODs include excessive tilt of the unit during high flow periods. Detection of non-target noise that results in % Time Lost was also greater for the SUB mounted C-POD. These tests of hydrophone performance inform the FORCE Environmental Effects Monitoring Program of the usefulness of sensor platforms in Minas Passage.

# Table of Contents

1.0	Introduction	5
1.1	Study Objectives .....	6
2.0	Filling Winter / Early Spring C-POD Data Gaps	7
2.1	Methods.....	7
2.2	Model Selection .....	9
2.3	Model Results .....	11
2.4	Descriptive Statistics.....	13
	Seasonal Trends at W1.....	13
	Julian Day .....	14
	Tidal Velocity .....	14
	Tidal Height .....	15
	Percent Time Lost.....	15
	Day Night Index (DNI).....	15
	Location .....	16
	Click Max.....	16
3.0	icListenHF Hydrophone Performance: Tank Tests	17
3.1	Hydrophone Calibration.....	17
3.2	Acoustic Foam Shroud Testing.....	17
3.3	In-tank Flow Tests .....	19
4.0	C-POD and icListenHF Hydrophone Performance: Field Tests	22
4.1	Introduction.....	22
4.2	Sensor Platform, Deployment and Recovery.....	22
4.3	Results.....	24
	C-POD Detections – SUBS vs. Platform.....	24
	C-POD Lost Time – SUB vs. Platform.....	26
	Mooring Unit Tilt – SUB vs. Platform .....	26
	C-POD and icListenHF Range Tests – Platform .....	27
	Effect of Shrouding on icListenHF Performance – Platform .....	29
5.0	General Discussion and Recommendations	31
6.0	References	33
7.0	Acknowledgements	34
8.0	Appendix	35

## List of Abbreviations and Symbols

AIC	Akaike Information Criterion
CCC	Concordance Correlation Coefficients
COSEWIC	Committee on the Status of Endangered Wildlife in Canada
C-POD	Chelonia - Porpoise Detector
dB	Decibel
DFO	Department of Fisheries and Oceans
DNI	Day Night Index
DPM	Detection Positive Minute (values 0 or 1)
DPMp10M	Detection Positive Minutes per 10 Minute period (values from 0-10)
DPM10M	Detection Positive 10 Minute period (values 0 or 1)
FFT	Fast Fourier Transform
FORCE	Fundy Ocean Research Center for Energy
GAM	Generalized Additive Model
GEE	Generalized Estimating Equation
Hz	Hertz
ICI	Inter Click Interval
kHz	Kilohertz
NBHF	Narrow Beam High Frequency
NOAA	National Oceanic and Atmospheric Administration
NSERC	Natural Sciences and Engineering Research Council
OERA	Offshore Energy Research Association
PAM	Passive Acoustic Monitoring
ppi	Pores per inch
re	Reference to
SALSA	Spatially Adaptive Smoothing Algorithm
SE	Standard error
sec	Second
SD	Standard Deviation
SD card	Secure Digital Card
SUB	Streamlined Subsurface Buoy
TISEC	Tidal In-Stream Energy Conversion
UTC	Coordinated Universal Time
VIF	Variance Inflation Factors
WUTS	Weak Unknown Transient Signals
10MP	10-minute period
$\mu$ s	Microsecond
$\mu$ Pa	Micro-Pascal

## 1.0 Introduction

Tidal power developments globally are currently focused on the testing of various large-scale commercial Tidal In-Stream Energy Conversion (TISEC) devices. Because there have been few installations to date, concerns remain regarding how TISEC device installation and operation will impact on marine life, especially marine mammals and fish (Langhamer et al., 2010). It is unknown if the noise produced during operation of in-stream tidal turbines will negatively affect marine mammals, but it is likely that each species will respond differently (Stewart et al., 2002). And, as the number of installed TISEC devices grows, the potential for negative impacts on marine animals (e.g. blade strikes) increases. In the early stages of testing TISEC devices, year-round pre-turbine installation baseline data are needed to assess how marine mammals naturally use tidal energy test sites. Post-installation monitoring will then allow detection of effects, if any.

The Fundy Ocean Research Centre for Energy (FORCE) is a TISEC test facility in Minas Passage, Bay of Fundy, where tidal energy developers can lease a designated berth (200 m diameter) to test and monitor their prototype devices and arrays. One of the main objectives of FORCE is to investigate environmental effects of TISEC operation, including effects of, and on, the environment (FORCE, 2012). This requires the collection of baseline data on the energy resource, the geophysical conditions and various biological components, including the use of the site by marine mammals. As the most commonly occurring marine mammal at the FORCE test site is the harbour porpoise (*Phocoena phocoena*) (OEER, 2008), they are the primary marine mammal species of concern in relation to TISEC operation.

Harbour porpoises can be effectively monitored with passive acoustic monitoring (PAM) devices because they are highly vocal and use echolocation (in the form of click trains) to gain perception of objects and landmarks for navigating, communicating and detecting prey. The frequency of echolocation click trains (duration of 75-150  $\mu$ s, beam angle of 15°) is between 100-160 kHz (Villadsgaard *et al.*, 2006). The maximum hearing sensitivity of harbour porpoises, based on audiograms, is between 100 and 140 kHz (Kastelein, *et al.*, 2002).

PAM devices are underwater microphones (hydrophones) that analyze and/or record sound (pressure differences) continuously over time. They are non-invasive, unaffected by weather, and monitor a specific area rather than an individual animal (Villadsgaard, 2006). Hydrophones monitor within limited distances from their moored locations and can record a large spectrum of sounds or can be specialized to detect specific sounds (e.g. porpoise click trains) based on pre-set characteristics. In this study, we used two hydrophone technologies (Figure 1.1) to monitor harbour porpoises in the Minas Passage: C-PODs (Chelonia Ltd.), which are porpoise detectors that detect click trains between 20-160 kHz, and the icListenHF hydrophone (Ocean Sonics Ltd.), which records sound from 0.01-204.8 kHz (Porskamp, 2013, Wood et al., 2013).

During the spring to fall periods of 2010-2012, multiple C-PODs were deployed at and near the FORCE turbine test site to examine harbour porpoise presence and activity for baseline purposes (Tollit et al., 2011; Wood et al., 2013). Porpoises were not expected to be present, at least not in high abundance, during winter. The current study tests that assumption. The new data fills a seasonal data gap and will be used to conduct full year statistical analyses (GAM/GEE) of the C-POD datasets and to update predictive models of porpoise presence (Wood et al., 2013). The outcomes will better inform current understanding of the seasonal trends and the determination of post-turbine installation changes in porpoise presence at and near the FORCE test site.



Figure 1.1. Hydrophone images. Top: C-POD (Chelonia Ltd). Bottom: icListenHF (Ocean Sonics Ltd).

## 1.1 Study Objectives

The main objective of this study was to close the winter/spring (Dec-May) baseline data gap via deployments of multiple C-PODs housed in SUB buoys (as in the prior multi-year study) at four selected monitoring locations and to reanalyze the year-round C-POD dataset for determination of trends in porpoise presence.

A secondary objective was the determination of the detection range and efficiency of two hydrophone types, the icListenHF (Ocean Sonics) and C-PODs (Chelonia Ltd.), over different current speeds during the tidal cycle at FORCE. Both instrument types have been successfully used in the Minas Passage (Tollit et al. 2011; Porskamp, 2013; Wood et al., 2013) but are known to be less efficient as flow noise increases. Quantifying this aspect of sensor performance has not been previously addressed.

Lastly, we tested an alternate mooring method (bottom instrument platform) for deploying autonomous C-POD and icListenHF hydrophones to assess and compare hydrophone detection performance under a range of flow and noise conditions, and to compare the detection performance of C-PODs housed in a tethered SUB buoy and a bottom moored instrument platform.

## 2.0 Filling Winter / Early Spring C-POD Data Gaps

### 2.1 Methods

To fill the seasonal data gap in prior harbour porpoise monitoring (Wood et al., 2013), C-PODs were deployed at four selected monitoring stations (E1, W1, W2 and S1) in and near the FORCE test site (Figure 2.1), from December 2013 to June 2014. This timeframe overlapped by one month (June) with previous spring to fall monitoring studies (2010-2012).

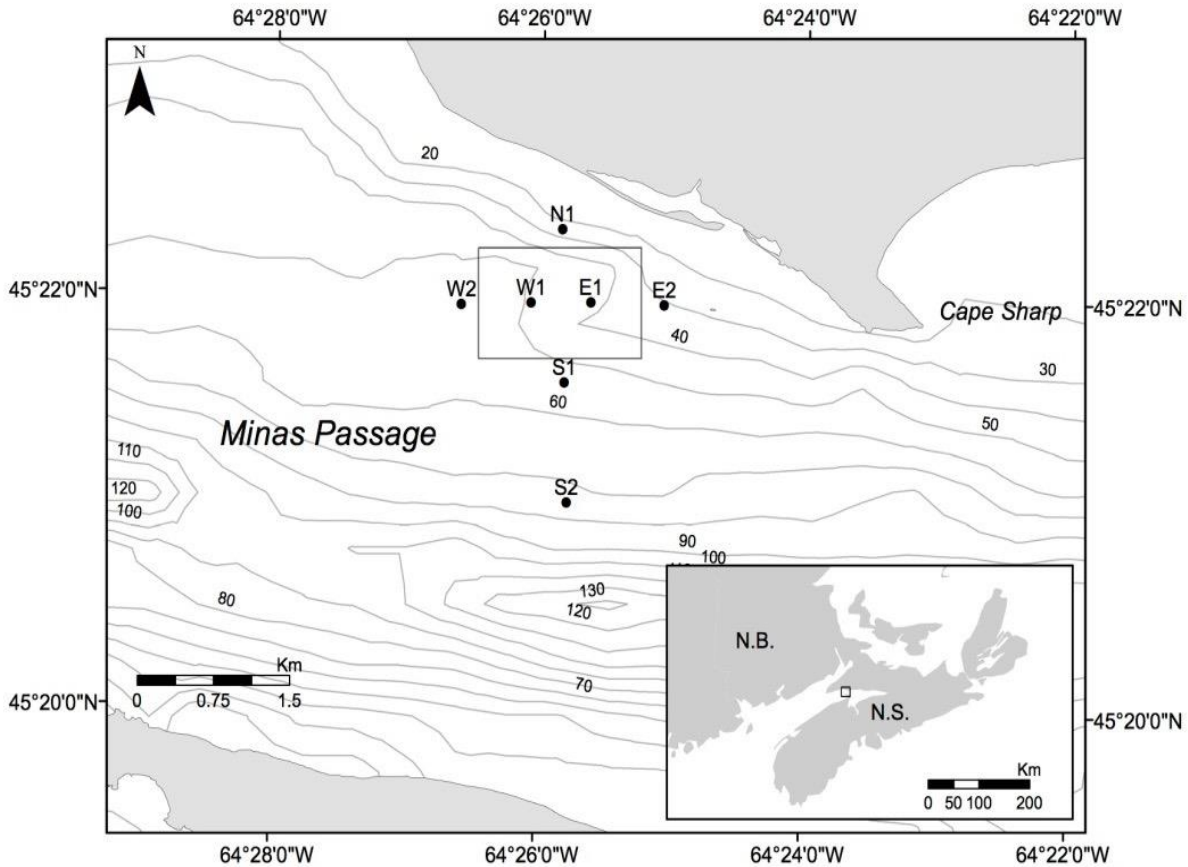


Figure 2.1. Bathymetric map of study location in Minas Passage, Nova Scotia, and multi-year (2010-2014) hydrophone stations at and near the FORCE test site. FORCE dimensions (rectangle) are 1.0 km x 1.6 km. Stations E2, S2 and N1 were not included in the current study. Depth contours are in meters.

In preparation for deployment in the Minas Passage, each C-POD was attached to the strongback of a Teledyne Benthos 875-T acoustic release and housed in a SUB buoy modified to fit the coupled sensors. The acoustic release of each unit was attached to a 2-3 m long, galvanized steel riser chain (1.27 cm diam.) and anchored with approximately 200 kg of large anchor chain links. Units were deployed from a chartered commercial lobster fishing vessel. The methodology of deployment and recovery is described in greater detail in Tollit *et al.* (2011).

On December 5<sup>th</sup> 2013, one C-POD was deployed at each of 4 monitoring sites; W1, W2, S1 and E1, with a duplicate C-POD deployed at W1. Batteries and memory cards were replaced for recovered C-PODs on April 2<sup>nd</sup> 2014. All units were recovered successfully except C-POD 639 (duplicate at W1). This unit was found on the shore near Parrsboro in May 2014 and returned to Acadia. After reviewing the tilt logs it was clear that the unit had released from its mooring the day after we attempted recovery. Due to unknown reasons (possibly battery clip issues) C-POD 1616 (Site E1) recorded for only 5 days. After battery and memory card exchanges, all recovered units were redeployed at their original stations and a spare C-POD (643) was deployed at W1 to replace C-POD 639. Recovery of these units took place on 2 July 2014.

After SD cards were downloaded the data were run through click classification software from Chelonia Ltd. (Software Version 2.043) to filter the data in order to distinguish between likely porpoise click-trains and other sounds detected by the C-POD. The software assessed and categorized each click-train by quality as questionable, low, moderate, or high probability that it was indeed part of a porpoise click-train. Moderate or high quality click-trains that are recorded within a minute are deemed a detection positive minute (DPM). This second stage (classification) determines the type of click-train (Delphinidae, Phocoenidae, other click-train source, boat sonar or unclassified) by assessing inter-click interval (ICI), frequency, and the length/amplitude of the click-train. Phocoenidae are represented by the class Narrow Band High Frequency (NBHF). Warnings are generated in the C-POD software when a high number of recorded clicks resemble Weak Unknown Transient Signals (WUTS). WUTS are unknown in origin but can resemble NBHF or dolphin clicks. Given the automated classification process, the post-processed data were assessed along with the original data to determine false positives and false negatives. All classified NBHF click trains (>1000) were examined for how intensity varied over the click train (the envelope). The false positives were mainly WUTS and sonar. After quality control was completed, the data were visualized in detection positive minutes (DPM) per day (Figure 2.2).



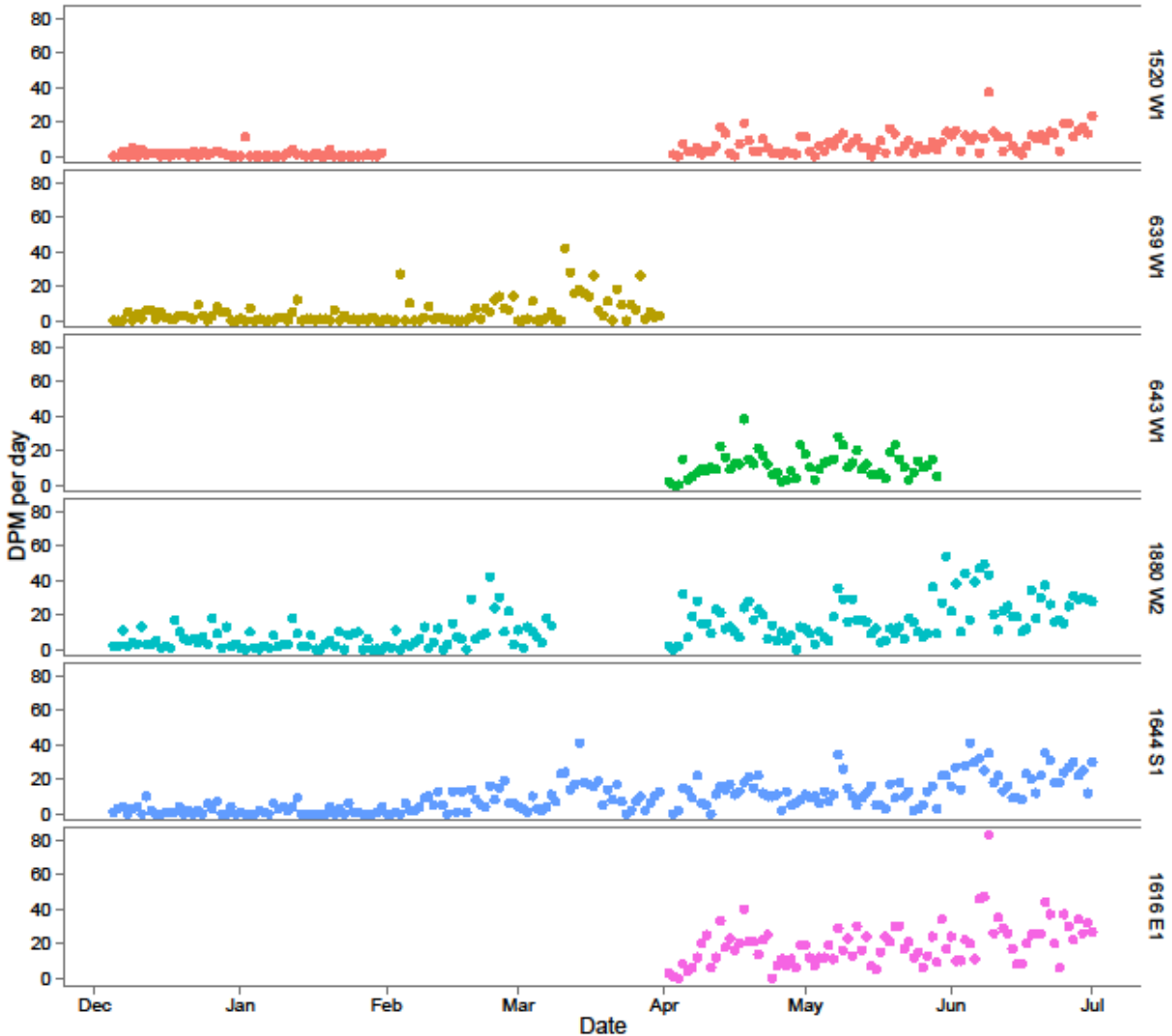


Figure 2.2. C-POD DPM per day for the 2013-2014 winter and spring deployments at sites WI, W2, S1 and E1. Coverage at site WI (top three panels) was duplicated for most of the study period. C-POD batteries and SD cards were exchanged on 2 April 2014.

## 2.2 Model Selection

The 2013-2014 winter / spring dataset was combined with datasets from previous monitoring years for a reassessment of harbour porpoise activity trends, using methods similar to those outlined in Wood *et al.* (2013). All statistical analyses were conducted using the computer package ‘R’ (R Core Team, 2014). The following packages were used in model creation: mgcv (Wood, 2014); geepack (Hojsgaard, *et al.*, 2006); splines (R Core Team, 2012); car (Fox and Weisberg, 2011); mvtnorm (Genz *et al.*, 2012); MRSea (Scott-Hayward *et al.*, 2014).

In order to interpret the full dataset, a GAM (General Additive Model) was built. A binary unit, DPM10M (detection positive 10 minute period), was used as the response. The response was modelled with a wide range of covariates inside GAM with logit link and binomial error. One assumption of a

GAM is that the model errors are independent. However, the errors in our dataset are not independent because the C-POD observations were collected close together with respect to time. The autocorrelation of error must be accounted for in the modelling approach. Since the raw data is zero inflated, it is likely that there will be a very low mean-variance relationship resulting in underestimation of the uncertainty around model estimates.

To account for autocorrelation the GAM created was run within a Generalized Estimating Equations (GEE) construct. GEEs can be used to account for temporal and spatial autocorrelation within a dataset. In order to facilitate the GEE the data within the model were grouped into panels such that data within a panel are assumed to be correlated while the data between panels is assumed to have independent error. The panel size was chosen using autocorrelation function plots. Autocorrelation results suggested that a panel size of 120 minutes would remove any autocorrelation present. This model structure provides identical coefficients to those of a standard GAM model, but the standard errors will differ under the GEE structure.

To determine if sensitivity varied between C-POD units, **C-POD ID** was included as a covariate in the models. **Location** at which C-PODs were deployed was included to determine spatial differences within the study area. **Area** was included to determine if detections in and out of the FORCE test site differed. **Click max** was included to determine if the setting had an impact on detection. Click max settings (4096 or 65536 depending on deployment) indicate the maximum number of “clicks” the C-POD can record over a one-minute period. If the number of clicks exceeds the set amount, the unit will stop recording for the rest of the minute. Click max ensures the memory card does not fill before the scheduled deployment period is over. To control for sediment noise and pseudonoise, we included **% Time Lost** (% of logging time lost due to minutes maxing out; this function is built in so that during times of high noise the C-POD’s memory card does not prematurely fill). **Julian Day** was included to determine if harbour porpoises detections exhibited seasonal patterns. **Temperature** was also included to determine if it had an effect on harbour porpoise patterns. To determine if porpoises within the Minas Passage exhibit diurnal patterns a **Day Night Index (DNI)** was included in the model. The DNI was a continuous index between 0 and 2. Values between 0 and 1 indicate daylight (dawn to dusk), values between 1 and 2 indicate night (dusk to dawn). Modelled **Tidal Velocity** and **Tidal Height** (Richard Karsten hydrodynamic model, Acadia University) were also included in the analysis to examine porpoise detection patterns in relation to velocity and tidal stage. Julian Day and DNI used circular splines since they are continuous variables which rollover: 365 to 1 for Julian Day, and 2 to 0 for DNI.

A GAM consists of multiple smoothing functions that connect together to form a curve. The location where one curve joins another curve is known as a knot. The number of knots and knot placement was determined using a Spatially Adaptive Smoothing Algorithm (SALSA). The MRSea package in R contains this algorithm and can apply SALSA in an automated process. The fitness measure chosen to compare models was the Akaike Information Criterion (AIC). Multiple models are generated and the calculated AIC of each model is compared to determine which knot placements produce the best model. The maximum iterations were set to 10 for each covariate. To ensure that all knots did not congregate around the same Julian Day, a gap of 15 days was chosen. Fifteen days produced better AIC values (i.e. closer to 0) compared to longer periods (30, 60, 90 days).

The initial GAM model failed to converge due to singularities. Singularities are caused by only one level of a covariate being present in a single level of another covariate (e.g. a single C-POD ID only being present in one location). Due to singularities both C-POD ID and Area were dropped. To avoid collinearity, the use of ‘variance inflation factors’ (VIF) was implemented using the vif function in the ‘car package’ in R. Large VIF values indicate collinearity. A common practice is to use a VIF threshold of 10, which was used in our model selection. Temperature was collinear with Julian Day and was therefore dropped from the model.

Of the seven covariates remaining, all seven were kept in the final model due to significant (i.e.  $p < 0.05$ ) GEE-based  $p$ -values. The relationship between each predictor variable and the response from the GAM/GEE model was plotted (Figure 2.3). The horizontal x-axis is the variable of interest for determining change in porpoise detections. The vertical y-axis explains how porpoise detection rates change as the variable of interest (x-axis) changes. The model plot **does not** depict actual DPM10M. The grey lines around splines and error bars depict 95% confidence intervals for the predicted relationships.

To determine the relative importance of each covariate in the model, the Concordance Correlation (CC) coefficients were calculated. Each time the model was run a covariate was removed. The covariate CC was compared to the full CC (whole model) and the differences in CC were used to rank the covariates (Table 2.1).

Table 2.1. Concordance correlation coefficients (CC) for the significant DPM10M covariates in the GAM/GEE model for all data collected (2011-2014). Based on CC values each covariate was ranked. See plots in Figure 2.3.

Covariate	Full CC	Covariate CC	Difference in CC	Rank
Julian Day	0.1128469	0.08392008	0.028926808	1
Tidal Speed	0.1128469	0.08440418	0.028442705	2
Tidal Height	0.1128469	0.08508366	0.027763227	3
% Time Lost	0.1128469	0.09499311	0.017853771	4
DNI	0.1128469	0.09915734	0.013689544	5
Location	0.1128469	0.10354926	0.009297627	6
Click Max	0.1128469	0.11070708	0.002139807	7

## 2.3 Model Results

The new GAM/GEE plots for the full dataset (2010-2014) show the largest peak in porpoise activity in late spring/early summer (June) followed by a smaller peak in the fall (late October) (Figure 2.3). Low porpoise detections are associated with mid-late summer and winter periods. The new model includes winter and early spring data which improves the original model predictions (Wood et al., 2013), as shown in the Appendix (Table A1 and Figure A1). Both the original and new GAM/GEE models show Julian day to be the most important covariate.

As expected, the GAM/GEE model predicts highest porpoise detection at low tidal velocities – at or near slack water (high and low tides) (Figure 2.3). At these times, ambient noise is low and thus % time lost is also low. Detections drop markedly at depth-averaged velocities  $> 2$  m/s. Tidal velocity ranks 2nd (out of 7) in importance as in the original GAM/GEE model.

The model predicts low porpoise detection at low tide heights (relative to mean height) in Minas Passage and high porpoise detection during periods of high tidal height (e.g. greater water depth).

% Time Lost is the fourth most important predictor. As it increases, porpoise detections decrease markedly. This covariate can be considered a proxy for current speed given that current-induced noise (e.g. bedload transport) causes the time lost effect.

Diel trends (Day Night Index or DNI) in porpoise detections were as expected. As in the original model, the lowest porpoise detection rates are associated with midday – early afternoon (DNI ~0.65); the highest detection rates are in the middle of the night (DNI of ~ 1.50) (Figure 2.3).

Porpoise detection rates vary across locations with higher detection rates in deeper waters (S1, 84 m) and lower detection rates at shallow depths (N1, 27 m) (Figure 2.3). All other stations are located at depths ranging from 40-60 m. Location results are similar to the original model.

The click max setting of 4096 resulted in greater predicted porpoise detections compared to using a click max setting of 65536 (Figure 2.3). After it was determined that the 65536 click max setting filled the memory cards too soon, and thus limited porpoise click train detections, this setting was no longer used. The higher click max setting was used for only 6% of the full dataset.

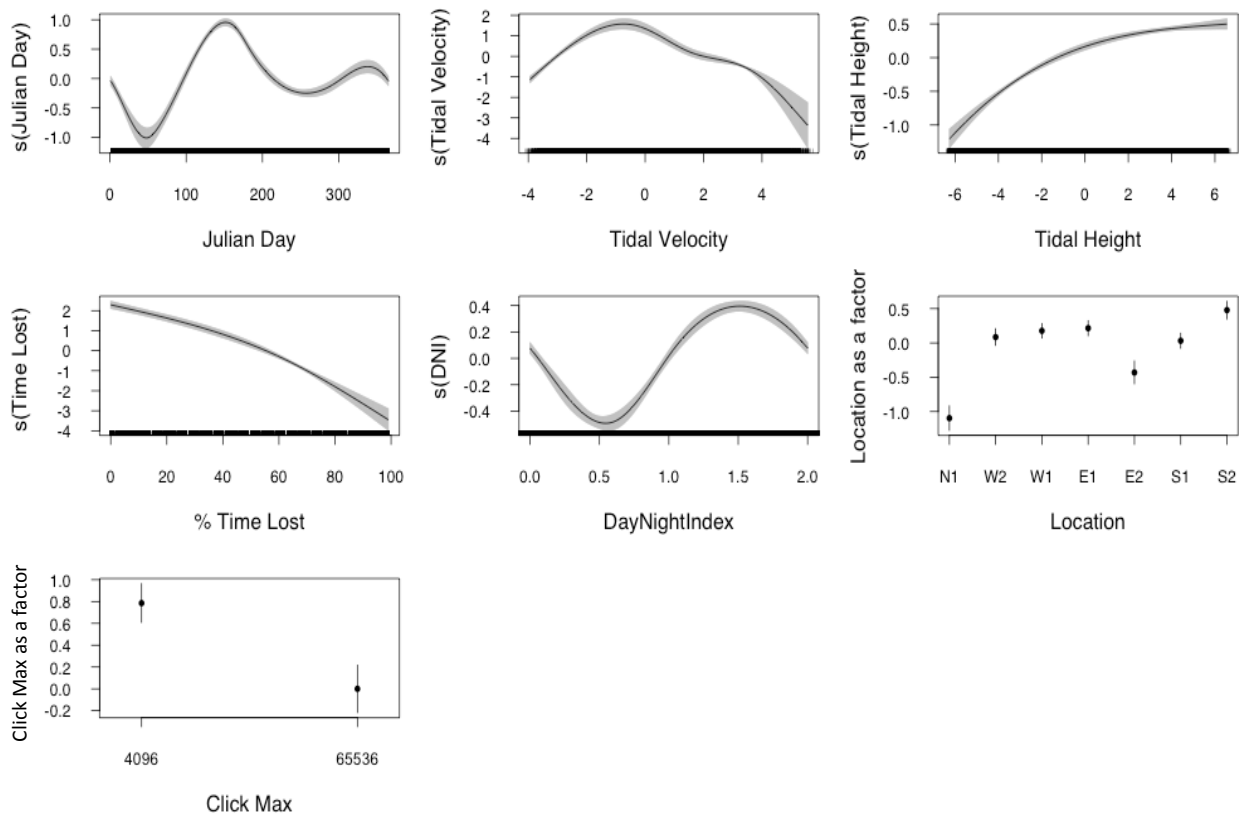


Figure 2.3. GAM/GEE plots of significant covariates and their relationship to porpoise DPM10M, in order of importance (see Table 2.1). Shaded areas and error bars represent 95% confidence intervals. Data includes all CPOD data collected during 2010-2014. For the Day Night Index, values between 0 (sunrise) and 1 (sunset) indicate daylight, values between 1 and 2 (sunrise) indicate night. Additional GAM/GEE models and plots that show trends in porpoise presence by season (winter, spring, summer, fall), time of day (day, night), and tidal stage (ebb, flood) can be found in Porskamp (2015).

## 2.4 Descriptive Statistics

### Seasonal Trends at W1

Because Location W1 (within the FORCE test area) has the most data and is the longest continuous monitoring location spanning all years of monitoring, it was chosen to highlight seasonal trends in porpoise detections at FORCE. Figure 2.4 and Table 2.2 show 30-day period trends in DPMp10M (Detection Positive Minutes per 10 Minute period; max=10) during winter, spring, summer and fall.

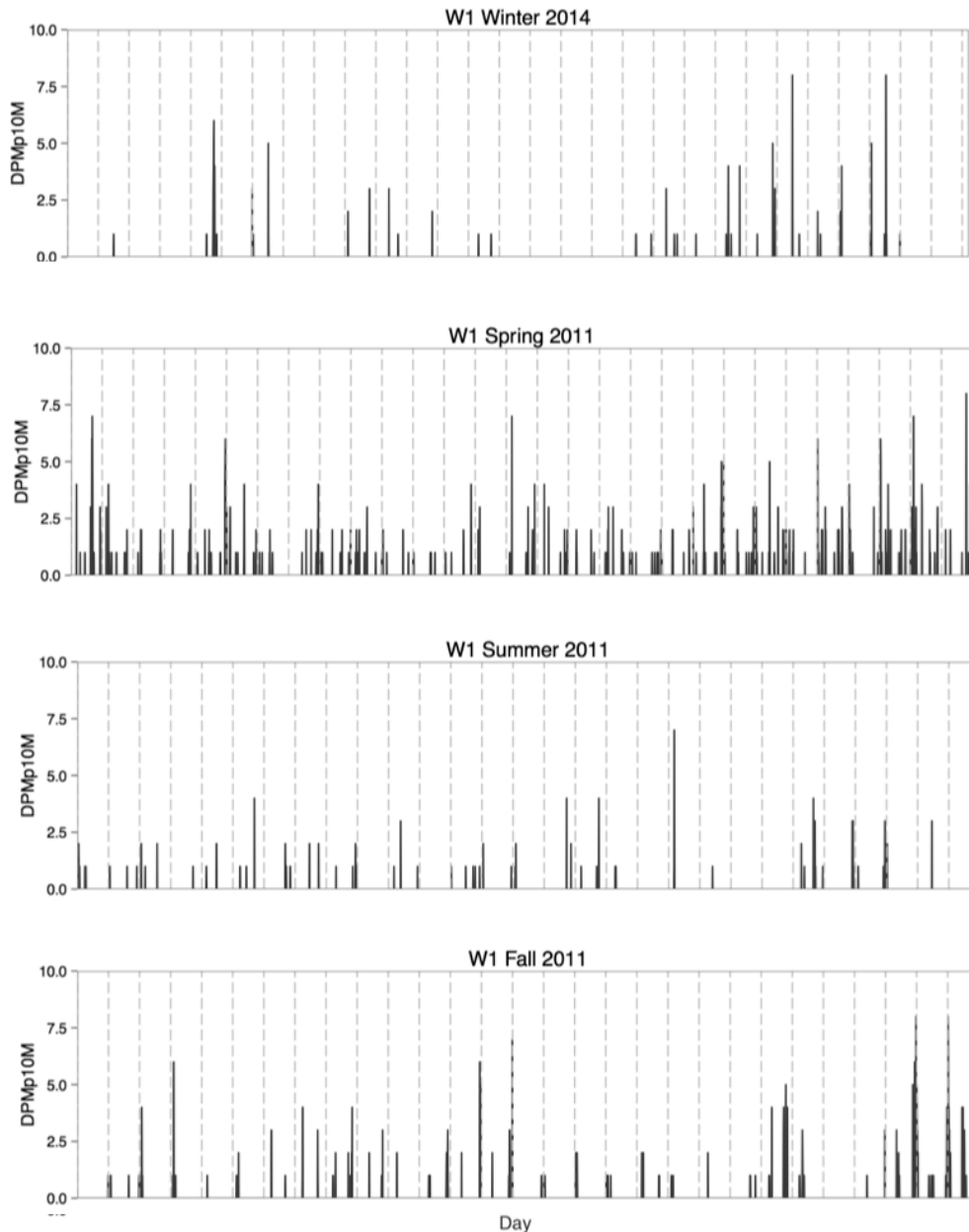


Figure 2.4. DPMp10M at location W1 highlighting detection trends across seasons and within months. Vertical dashed lines indicate the start of a new day (i.e. midnight). Spring, summer and fall plots are from Wood et al. (2013). See Table 2.2 for Julian Day periods.

The results concur with the GAM/GEE model, which predicts spring to have the most DPMp10M and winter to have the lowest. Summer and winter detections are irregular on a temporal scale and are most likely driven by how porpoises are using the Minas Passage during those seasons. Detections are most common during the hours just before and after midnight (vertical dashed lines).

The following sections include all sites and describe the statistics for each covariate but should be interpreted with care. This is because the data is zero inflated (many zeros throughout the dataset) and the standard deviation is large. Median and mode cannot be used because in most cases they would be 0. Regardless, the model outcomes (Figure 2.3) reflect well the collected data, as shown in Tables 2.2-2.8.

### **Julian Day**

The spring peak (May/June) in DPMp10M is 1.5 times the fall peak, with winter and summer being considerably lower (Table 2.2). Note the winter sample size of 10 minute periods (10MP) is smaller because there is only one year of data (2014) and not two or more as with all other seasons. The GAM/GEE model and descriptive statistics show similar trends.

Table 2.2. Descriptive statistics for periods of 30 Julian Days corresponding to spring, summer, fall and winter periods as shown in Figure 2.4. The % of 10MP with DPM is the percentage of 10-minute periods with at least one porpoise detection. \* 1 year of winter data only.

<b>Julian Day Range (season)</b>	<b>Dates</b>	<b>Mean DPMp10M</b>	<b>SD</b>	<b>% of 10 MP with DPM</b>	<b>No. of 10MP</b>
30-60 (winter)	30 Jan – 1 March	0.05	0.38	2.1	13392*
130-160 (spring)	10 May – 9 June	0.12	0.59	6.6	45055
220-250 (summer)	8 Aug – 7 Sept	0.03	0.27	1.8	34735
280-310 (fall)	7 Oct – 6 Nov	0.09	0.55	4.1	41670

### **Tidal Velocity**

Descriptive statistics for tidal velocity suggest that the highest porpoise presence is associated with low current velocities on the ebb tide (-2 to 0 m/s) (Table 2.3). Trends here are not taking into account % time lost, which occurs at high flow velocities, especially on the flood tide. The sample size for fast flood currents (depth average speed >2 m/s) is 2x larger than fast ebb currents because flood tidal currents exceed 2 m/s for longer periods.

Table 2.3. Descriptive statistics for four Tidal Velocity classes (depth-averaged velocity). The % of 10MP with DPM is the percentage of 10-minute periods with at least one porpoise detection.

<b>Velocity (m/s) (tidal stage)</b>	<b>Mean DPMp10M</b>	<b>SD</b>	<b>% of 10 MP with DPM</b>	<b>No. of 10MP</b>
-4 to -2 (fast ebb)	0.05	0.36	3.0	34767
-2 to 0 (slow ebb)	0.14	0.66	6.6	97669
0 to 2 (slow flood)	0.06	0.41	3.5	79522
2 to 4 (fast flood)	0.04	0.34	2.0	71655

### **Tidal Height**

The GAM/GEE model plots (Figure 2.3) suggest that porpoise detections are highest at high tide levels (relative to mean tide height) and lowest at low tides. The descriptive statistics also show an increase in porpoise presence as tidal height increases (Table 2.4)

Table 2.4. Descriptive statistics for five tidal height classes. A tidal height of zero is the mean tidal height in Minas Passage. The % of 10MP with DPM is the percentage of 10-minute periods with at least one porpoise detection.

<b>Tidal Height (m) Relative to Mean Tidal Height</b>	<b>Mean DPMp10M</b>	<b>SD</b>	<b>% of 10 MP with DPM</b>	<b>No. of 10MP</b>
-6 to -4	0.05	0.38	2.8	41773
-4 to -2	0.06	0.40	3.2	65213
-2 to 2	0.06	0.46	3.1	85161
2 to 4	0.10	0.56	5.3	54713
4 to 6	0.15	0.64	7.3	42448

### **Percent Time Lost**

When the minute memory limit fills prior to 60 sec, the remaining detection time within that minute is lost. This effect occurred during 36% of the 10 MPs in the full dataset. Not surprisingly, lost time has an effect on porpoise detection rates with detections decreasing as % lost time increased (Table 2.5). The GAM/GEE model (Figure 2.3) shows a similar pattern.

Table 2.5 Descriptive statistics for four classes of % Time Lost. The % of 10MP with DPM is the percentage of 10-minute periods with at least one porpoise detection.

<b>% Time Lost</b>	<b>Mean DPMp10M</b>	<b>SD</b>	<b>% of 10 MP with DPM</b>	<b>No. of 10MP</b>
0-25	0.10	0.56	5.4	207996
25-50	0.03	0.28	1.8	8403
50-75	0.01	0.13	0.6	12969
75-99	0.00	0.07	0.1	54164

### **Day Night Index (DNI)**

Daylight periods were associated with lower harbour porpoise detections, based on DPMp10M, than nighttime periods (Table 2.6). The GAM/GEE model showed a similar pattern.

Table 2.6. Descriptive statistics for four Day Night Index classes. The % of 10MP with DPM is the percentage of 10-minute periods with at least one porpoise detection. DNI values of 0 and 2 represent sunrise and an index value of 1 is sunset.

Day Night Index	Mean DPMp10M	SD	% of 10 MP with DPM	No. of 10MP
0.0 to 0.5	0.07	0.43	3.7	75379
0.5 to 1.0	0.06	0.38	3.2	75427
1.0 to 1.5	0.09	0.54	4.4	68136
1.5 to 2.0	0.11	0.59	5.2	69397

### Location

As with the GAM/GEE model, detection statistics for location (Table 2.7) show low porpoise presence in the shallowest location (N1, 27 m) and highest detections at the deepest site (S2, 84 m). All other locations are between 40 and 60 m in depth and have similar detection rates except for E2, which is located near Black Rock and exhibits extremely high levels of ambient noise (i.e. high % lost time).

Table 2.7. Descriptive statistics for the seven monitoring locations (see Figure 2.1). % of 10MP with DPM is the percentage of 10-minute periods with at least one porpoise detection. Sites in the FORCE test area are in bold.

Location (m)	Mean DPMp10M	SD	% of 10 MP with DPM	No. of 10MP
N1 (27)	0.03	0.26	1.3	26212
W2 (59)	0.09	0.49	4.7	30275
<b>W1 (56)</b>	<b>0.09</b>	<b>0.55</b>	<b>4.5</b>	<b>78816</b>
<b>E1 (52)</b>	<b>0.11</b>	<b>0.56</b>	<b>5.3</b>	<b>67186</b>
E2 (41)	0.04	0.36	1.7	24213
S1 (59)	0.07	0.42	3.6	51152
S2 (84)	0.11	0.52	6.4	13774

### Click Max

As the model predicts, porpoise detection rates were higher with a click max of 4096 than with a click max of 65536 (Table 2.8). However, as click max settings represent different deployment periods, results should be interpreted with care.

Table 2.8. Descriptive statistics for the two Click Max settings used in this study. % of 10MP with DPM is the percentage of 10 minute periods with at least one porpoise detection.

Click Max	Mean DPMp10M	SD	% of 10 MP with DPM	No. of 10MP
4096	0.08	0.50	4.2	271500 (94%)
65536	0.04	0.32	2.4	16950 (6%)



### 3.0 icListenHF Hydrophone Performance: Tank Tests

During the spring of 2014, tests were conducted to compare the porpoise detection performance of C-PODs and icListenHF hydrophones in Minas Passage. Prior to the field tests, two icListenHF hydrophones were calibrated. Various acoustic shroud materials were then tested for effectiveness in reducing flow noise at the sensor tip (pseudonoise).

#### 3.1 Hydrophone Calibration

All icListenHF hydrophone calibrations were conducted at the Ocean Sonics Ltd facility in Great Village, Nova Scotia. Calibration results are shown in Figure 3.1 for hydrophones 1211 and 1239, both with custom made high-density polyethylene (HDPE, engineered plastic) guards (Figure 3.2). Hydrophone 1211 was slightly more sensitive in the range of porpoise echolocation frequency (130 kHz) compared to hydrophone 1239. However, hydrophone 1211 was less sensitive at higher and lower frequencies compared to hydrophone 1239.

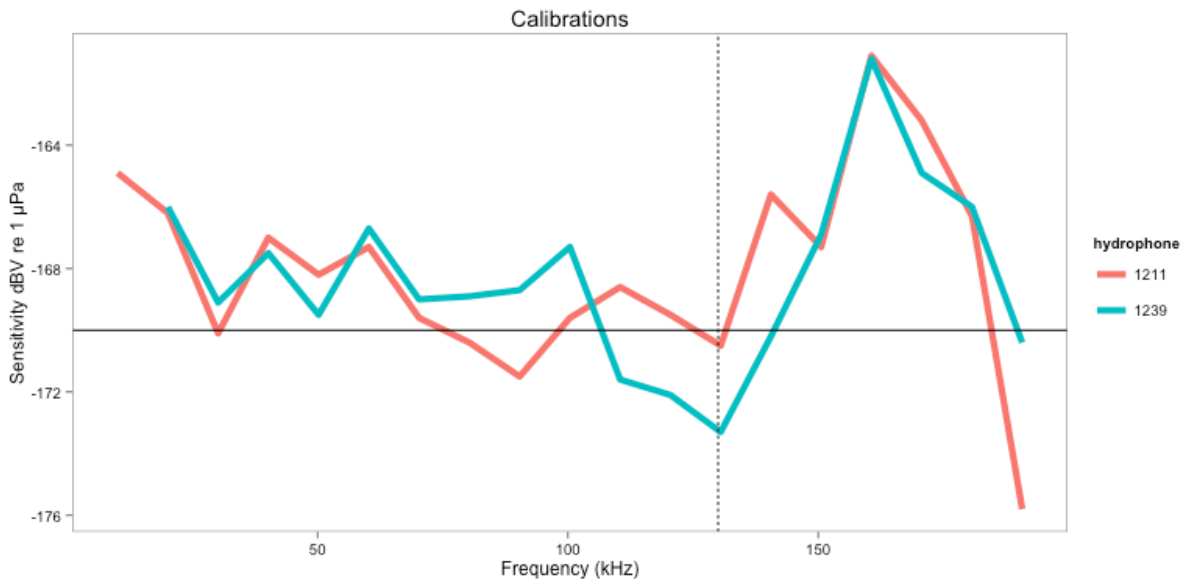


Figure 3.1. Calibration results for icListenHF 1211 and 1239 fitted with HDPE guards. Horizontal bar is a reference at -170 dBV re 1µPa. Vertical dashed line (130 kHz) is within the harbour porpoise echolocation frequency range (100-160 kHz).

#### 3.2 Acoustic Foam Shroud Testing

The effect on performance of the icListenHF hydrophone when it is shrouded with acoustic foam was tested using foam densities of 20 ppi (pores per inch), 30 ppi and 40 ppi, and with three different foam thicknesses: 0.5 inch, 1.0 inch and 1.5 inch. All shroud plus guard setups were calibrated except for the 40 ppi foam because this foam type attenuated all sound. All calibrations were conducted in a semi-spherical (2.4m diameter by 1.2m deep) round-bottom calibration tank, filled with fresh water, at the Ocean Sonics Ltd facility. The tank was located in an elevated hut lined with insulation to ensure a quiet environment. Calibrations (relative) were conducted using a RESON hydrophone paired with an icListenHF hydrophone. An icTalk speaker was used to generate a series of sound sweeps in 10 kHz

steps, 1m from the hydrophone. The icListenHF was then adjusted to match the RESON hydrophone sensitivity.

icListenHF 1211 was selected as the control unit because the initial calibration showed it was more sensitive at 130 kHz when compared to icListenHF 1239 (Figure 3.1). Calibration results for various shroud setups with hydrophone 1239 are shown in Figure 3.3. The shroud setup using 20 ppi attenuated low frequency sounds and was the best performing acoustic foam type for preserving higher frequency sounds. As thickness of the 20ppi foam increased, the amount of attenuation increased. The shroud setup using 30 ppi attenuated high frequencies while preserving the lower frequencies.



Figure 3.2. IcListenHF hydrophone tip with custom made HDPE guard (left) and with 0.5 inch, 20 ppi foam cover secured over the guard (right).

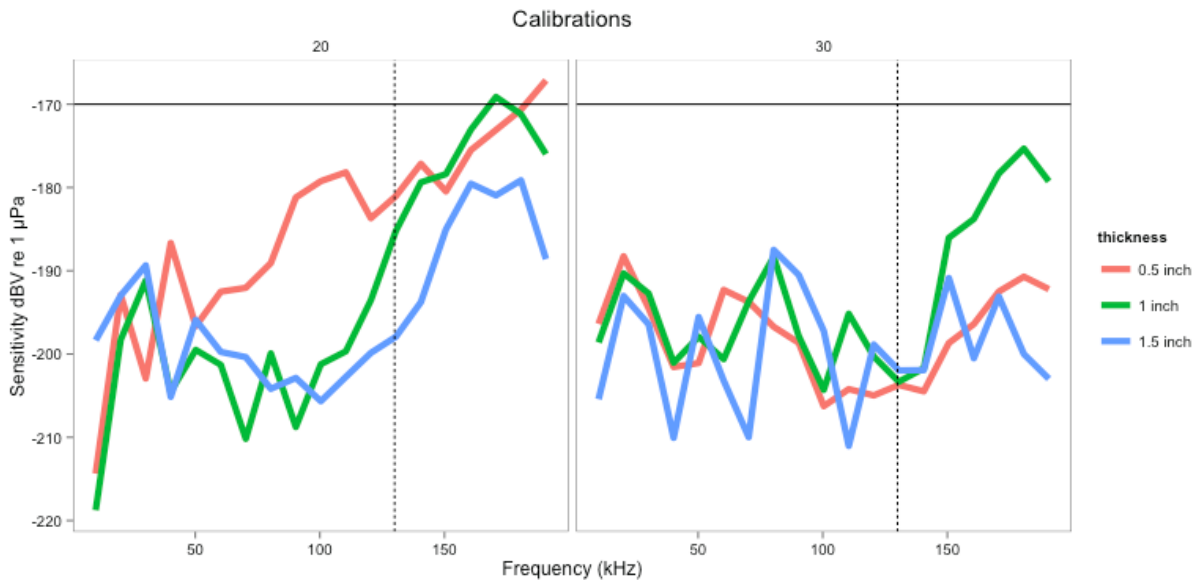


Figure 3.3. Calibration results for icListenHF 1239 for various foam thicknesses (0.5, 1.0 and 1.5 inch) and pore density. **Left:** 20 ppi foam. **Right:** 30 ppi foam. Horizontal bar is a reference at -170 dBV re 1µPa. Vertical dashed line (130 kHz) is within the frequency range that porpoises use for echolocation.

The shrouded hydrophone calibration tests showed that two setups (20 ppi foam, at both 0.5 inch and 1.0 inch thicknesses) attenuated sound at low frequencies while maintaining sensitivity at higher frequencies (e.g. porpoise click train). These options were selected for flow testing (1 m/s).

### **3.3 *In-tank Flow Tests***

To generate flow in the tank, a custom-made flow wheel was attached to the ceiling of the calibration hut. The hydrophones were attached to the arms of the flow wheel and submerged to a depth of 30cm. Each hydrophone recorded ambient noise for two minutes so that the noise floor could be determined before testing commenced. To avoid any impact of motor noise, the flow wheel was powered by two people pulling in opposite directions on a rope coiled around the axle of the flow wheel. Three trials were conducted under flow speeds of about 1 m/s for 30s. Each setup was tested five times. The hydrophone setups for flow testing were: guard only, guard with 0.5 inch 20 ppi foam cover, and guard with 1.0 inch 20 ppi foam cover.

An icTalk speaker (Ocean Sonics Ltd) was used during the tank flow tests to produce a sound sweep from 120 kHz to 140 kHz at 120 dB re 1 $\mu$ Pa. The sweep duration was 0.1 s with a 0.9 s rest. The sweep was designed to mimic a porpoise click train without ICIs (Figure 3.4 & 3.5).

Pseudo-noise (flow noise) was observed for both shrouded and non-shrouded hydrophones at all frequencies although primarily between 0 – 80 kHz (Figure 3.4). Noise above 100 kHz may be due to a phenomenon known as “thermal noise” which is caused by water particles striking the hydrophone tip (Urick, 1984). As expected, at higher foam thickness, attenuation increased at all frequencies.

The software program, RavenPro 1.4, was used to compare shrouded and non-shrouded hydrophones datasets. The frequency bins impacted by flow noise were manually selected and the dB re 1  $\mu$ Pa was calculated. Compared to the control hydrophone (with guard but non-shrouded), 0.5 inch 20 ppi foam reduced sweep intensity by 10 dB  $\pm$  2 dB, and reduced flow noise by 30 dB  $\pm$  4 dB. The 1.0 inch foam reduced sweep intensity by 20 dB  $\pm$  3 dB, and reduced flow noise by 30 dB  $\pm$  5 dB, across all frequencies impacted by flow noise. Because the 0.5 inch foam had the least impact on sweep intensity, this foam thickness was selected for a field deployment in Minas Passage.

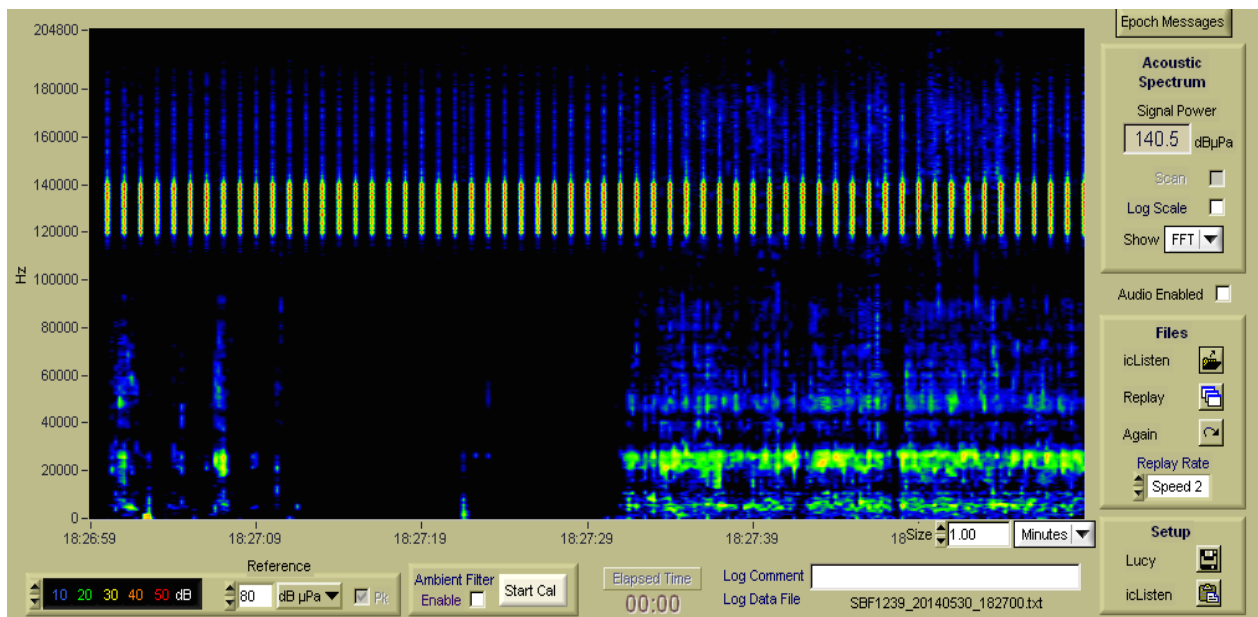
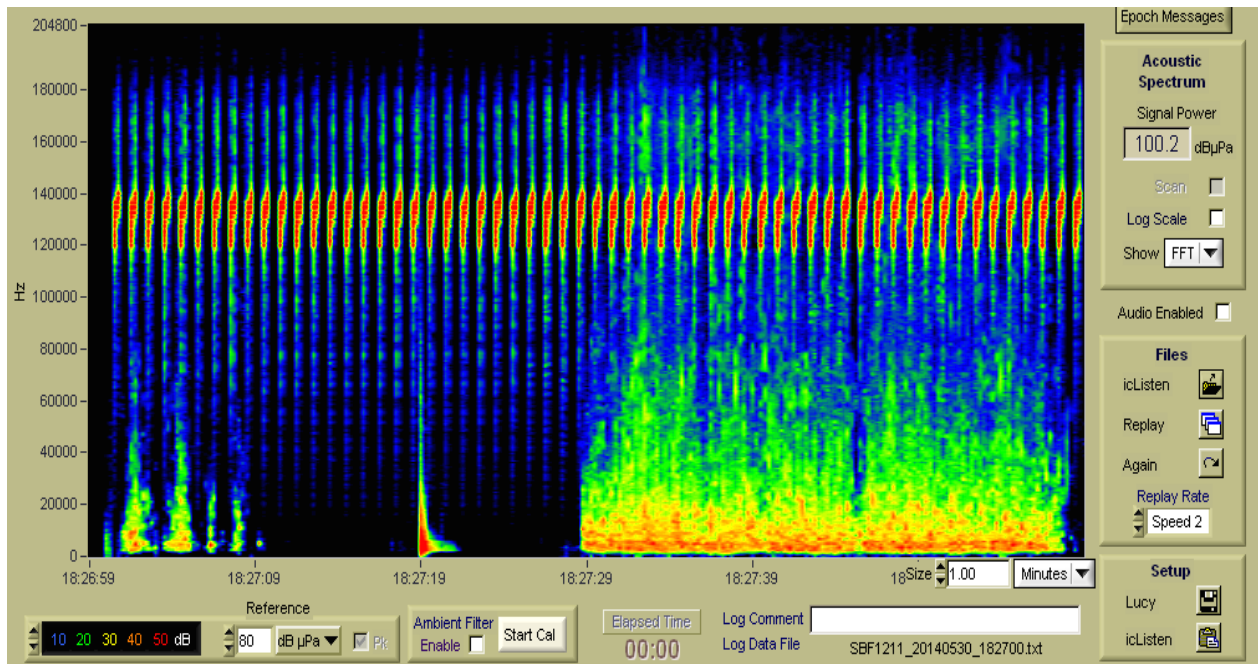


Figure 3.4. *IcListenHF* spectrograms from tank test trials. **Top:** without acoustic foam. **Bottom:** 0.5 inch thick, 20 ppi acoustic foam. The tank test trial commenced half way through the minute. FFT update rate 4/s.

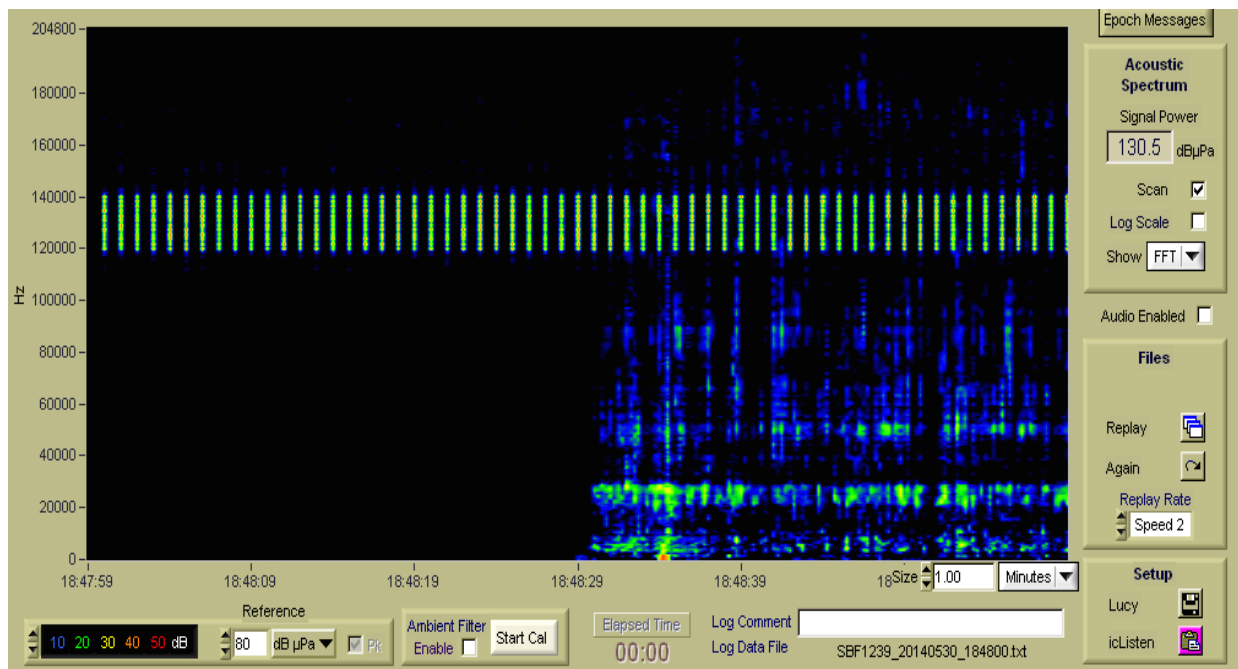
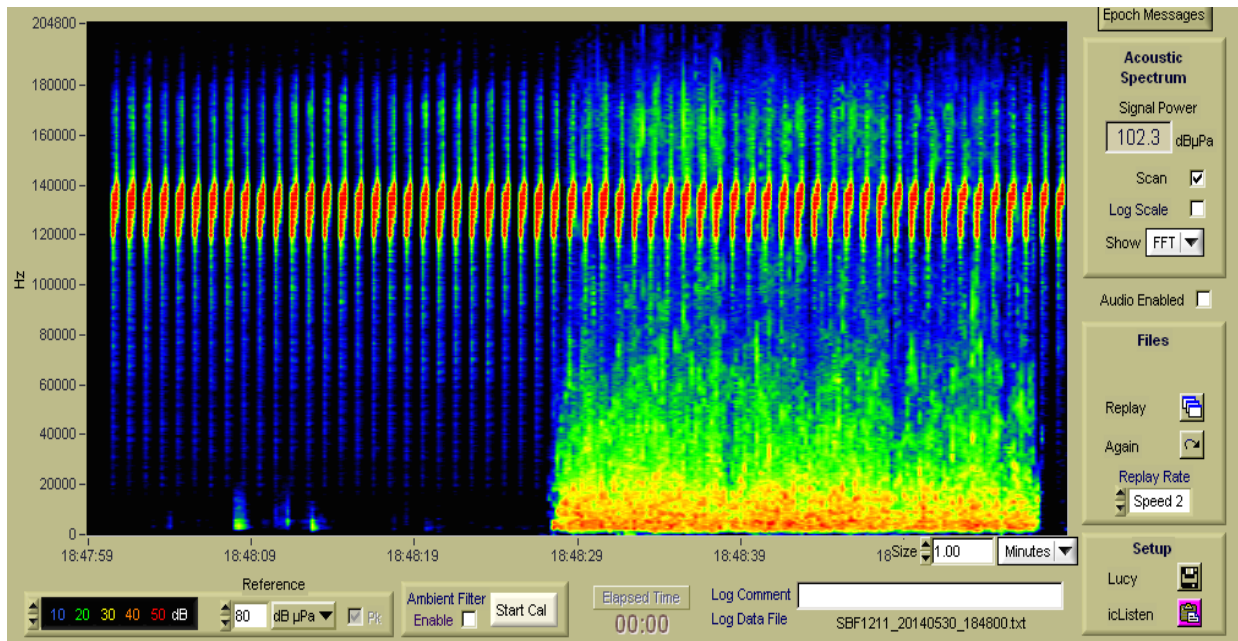


Figure 3.5. IcListenHF spectrograms from tank test trials. **Top:** without acoustic foam. **Bottom:** 1.0 inch thick, 20 ppi acoustic foam. The tank test trial commenced half way through the minute. FFT update rate 4/s.

## 4.0 C-POD and icListenHF Hydrophone Performance: Field Tests

### 4.1 Introduction

Since 2010, all PAM studies of harbour porpoise in the Minas Passage have employed SUB buoys (Open Seas Instrumentation Inc.) (Tollit et al., 2011; Wood et al., 2013). SUB buoys have internal floats housed within a streamlined casing that swivels to align with current direction (Figure 4.1). For this study, SUB buoys were tethered about 2-3 m above the seafloor. Roughly 200 kg of large chain links are used as an anchor to prevent moored units from moving off site during high flow periods. A hydrophone and a Teledyne Benthos 875-T acoustic release for recovery are housed within the mid-section of the SUB buoy. The use of acoustic releases eliminates the need for a surface buoy, and thus reduces drag and risk of mooring displacement. This configuration has been previously used to house both C-PODs and an icListenHF. The battery pack for the icListenHF, however, caused significant tilt under high flow conditions (Porskamp, 2013), which may have resulted in increased noise and reduced detection of harbour porpoises.

In an attempt to reduce tilt effects and non-target noise, this project tested the performance of C-PODs and icListenHF hydrophones (with and without an acoustic foam shroud), mounted to a bottom standing instrument platform (lander) (Figure 4.2).

### 4.2 Sensor Platform, Deployment and Recovery

The instrument platform (also referred to as a lander) was fitted with an acoustic release (ORE Sport Release), temperature logger, pressure logger, two tilt loggers, two VEMCO VR2Ws (used for another project), two icListenHF hydrophones, two C-PODs, and approximately 400 kg of anchor weight (Figures 4.1 and 4.2). The sensors were located about 1 m off the seafloor, within the boundary layer where current speeds are reduced (<1 m/s). A spool of high tensile strength rope and two VINYL ball floats were attached to the platform. Triggering of the acoustic release uncoils the rope enabling the floats to rise to the surface to allow platform recovery. The backup recovery system comprised a low drag surface buoy attached via rope to a safety anchor (200 kg of large anchor chain), connected to the platform via a 100 m stainless steel cable.

The instrument platform was deployed at station W1 (Figure 2.1) on 5 June 2014 and recovered from Minas Passage on 2 July 2014. During deployment a Teledyne Benthos 866-a acoustic release that was used to lower the platform failed to release. As a result, a second charter (12 June) was required to pull the platform up and manually remove the acoustic release. At this time, all sensors were inspected and it was noted that the icListenHF 1211 guard arm (protective cage) was cracked but still attached at the base. The platform was successfully redeployed using a  $\frac{3}{4}$  inch rope running through a shackle attached to the platform. The damage was most likely caused by the failed acoustic release making contact with the sensors at high flow speeds during the 1<sup>st</sup> week of deployment. The temperature, pressure and tilt loggers performed as expected.

Upon recovery of the platform on 2 July, it was noted that one of the 2 co-located C-PODs (1615) was missing (reason unknown). It was later found on the shore near Parrsboro, NS and returned to Acadia in December 2014. The dataset indicated that it became detached from the platform on 12 June, most likely during the redeployment of the platform. Both icListenHF hydrophones were inspected by Ocean Sonics Ltd. for damage and recalibrated. By comparing the noise floor pre and post deployment it was determined that the entire dataset collected by icListenHF 1239 throughout the deployment period was

valid (per. comm. David Sampson). The tip of icListenHF 1211 was damaged; the stored data were inspected by looking at the noise floor changes in all spectrograms. It was concluded that, after 7 days of successfully recording data, the hydrophone sustained damage and all further data were considered not valid (per. comm. David Sampson). Analyses of the data collected by unit 1211 included only the first 7 days of the deployment period.

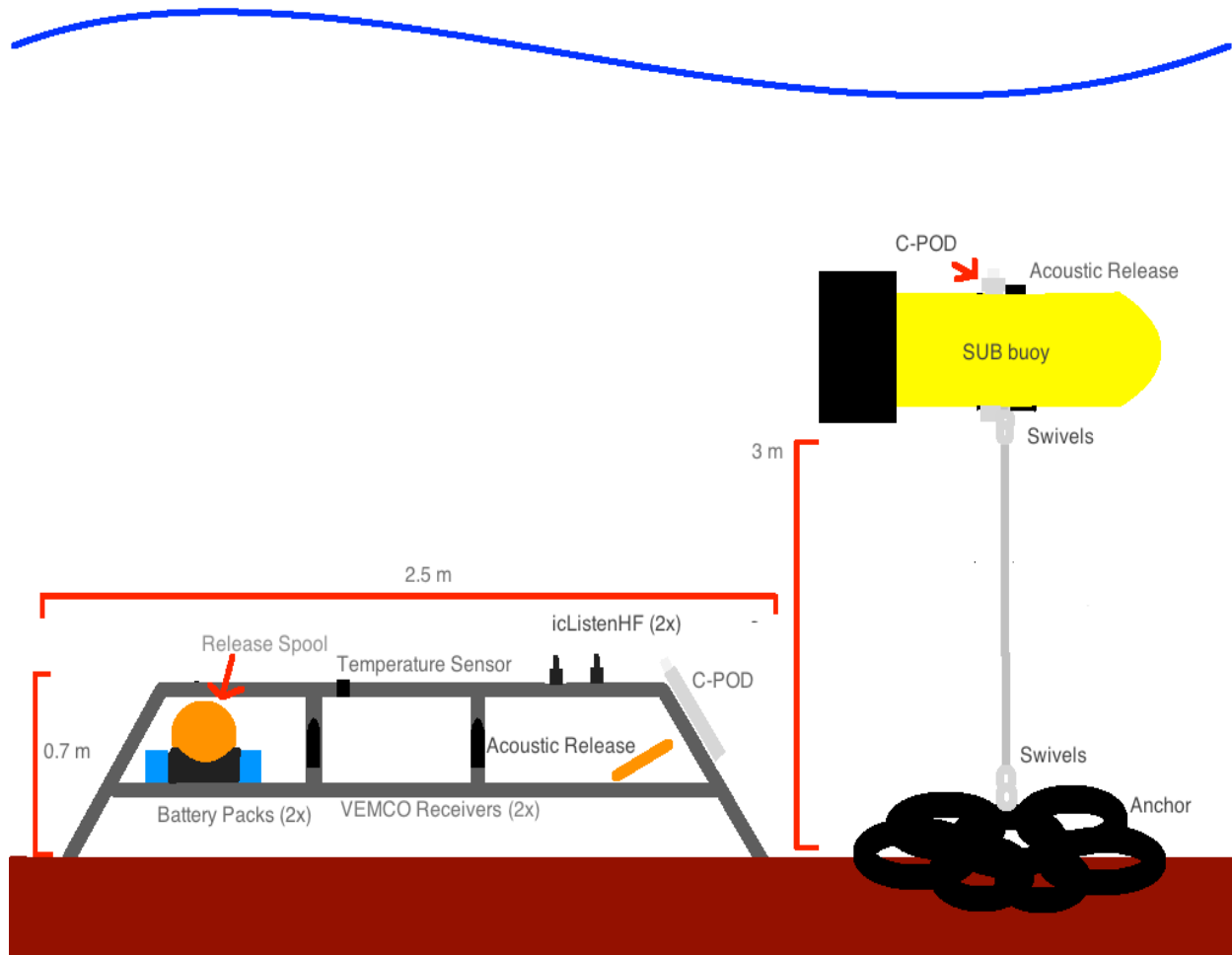


Figure 4.1. Mooring designs. **Left:** Instrument platform housing two icListenHF hydrophones with battery packs, a C-POD, and an acoustic release, plus other sensors (temperature, VEMCO receivers). **Right:** SUB buoy housing an acoustic release and a C-POD, and attached to anchor weight (about 200 kg) with a 3 m long riser chain.



Figure 4.2. Image of instrument platform prior to deployment. Note the 2 C-PODs in the far corners and the shrouded and non-shrouded icListenHF hydrophones (black sensors) located above their battery packs. The instrument hanging vertically above the frame is the Teledyne Benthos 866-a acoustic release.

### 4.3 Results

#### C-POD Detections – SUBS vs. Platform

Harbour porpoise DPM/day were calculated for the platform mounted C-PODs and the two SUB buoy mounted C-PODs located at W1 (up to 30 m apart). Only moderate and high quality click trains were considered for comparison. The platform mounted C-PODs detected greater numbers of click-trains and greater detection positive minutes (DPM/day) compared to the co-located, SUB buoy-mounted CPODs (Table 4.1, Figure 4.3). Platform mounted C-PODs 639 and 1615 showed similar detection peaks in early June after which C-POD 1615 became detached from the platform.



Table 4.1. C-POD detection results from co-located units at station location W1 during 5 June to 2 July 2014. Of the two C-PODs moored in SUB units, C-POD 643 prematurely stopped recording on 1<sup>st</sup> June 2014. Two C-PODs were housed on the instrument platform; C-POD 1615 unexpectedly detached from the platform on 13<sup>th</sup> June 2014.

C-POD unit	Deployment Method	Detection Start / End Dates	Detection Duration	DPMs recorded (mean/day)
1520	SUBS	5 June / 2 July	30d 00h 00m	251 (8.3)
639	Platform	5 June / 2 July	30d 00h 00m	378 (12.6)
1615	Platform	5 June / 13 June	8d 13h 26m	85 (10.4)

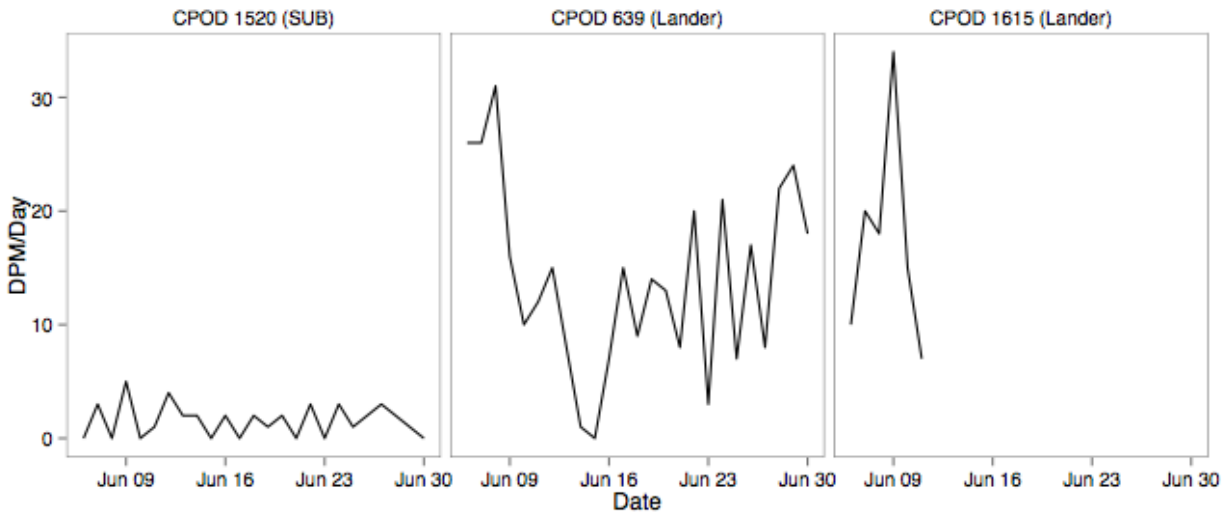


Figure 4.3. DPM/Day of SUB buoy mounted C-POD 1520 and platform (lander) mounted C-PODs 639 and 1615 (detached on June 12<sup>th</sup>). No data are available for SUB buoy mounted C-POD 643 for this period because this unit stopped functioning on 1 June 2014.

### **C-POD Lost Time – SUB vs. Platform**

Percent lost time (due to excessive ambient noise) for the SUB buoy housed C-POD (1520) and platform mounted C-POD (639) was similar during flood tides (Figure 4.4). During the ebb tides, lost detection time was lower for the platform attached C-POD, especially during neap tidal cycles. A Wilcoxon signed rank test ( $\alpha = 0.05$ ) with continuity correction compared the two datasets and returned a p-value of  $<0.001$  indicating that C-POD 1520 (SUB buoy) lost significantly more detection time than C-POD 1615 (platform).

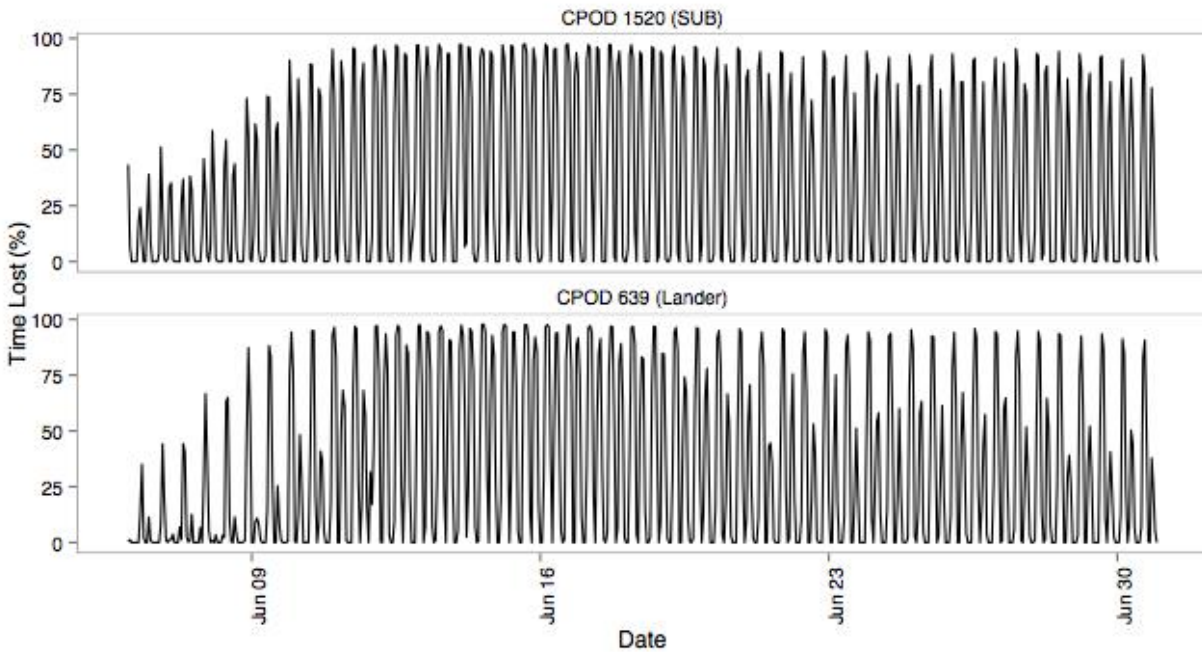


Figure 4.4. C-POD percent lost time plots. **Top:** SUB Buoy mounted C-POD 1520; **Bottom:** platform mounted C-POD 639. The series of peaks represent the sequence of flood and ebb tides during June 2014 with flood tides showing greater % lost time compared to ebb tides. A spring-neap pattern is also evident; a full moon occurred on 13th June 2014.

### **Mooring Unit Tilt – SUB vs. Platform**

Data were successfully retrieved from two HOBO Pendant G Data Tilt Loggers (UA-004-64) housed on both the platform and a co-located SUB buoy. The tilt loggers were set up perpendicular to each other in order to record both pitch and roll. The units sampled tilt at 5-minute intervals. The mean tilt for the deployment period for each axis was calculated and set as a reference.

During the deployment period (June 2014), the platform tilt sensor exhibited very little movement in both the pitch (z.tilt) and roll (y.tilt). In contrast, the SUB buoy showed up to 60 degrees on the pitch during the flood tide and 25 degrees on the roll, with tilt greater at depth-averaged flow speeds exceeding 1 m/s (Figure 4.5).

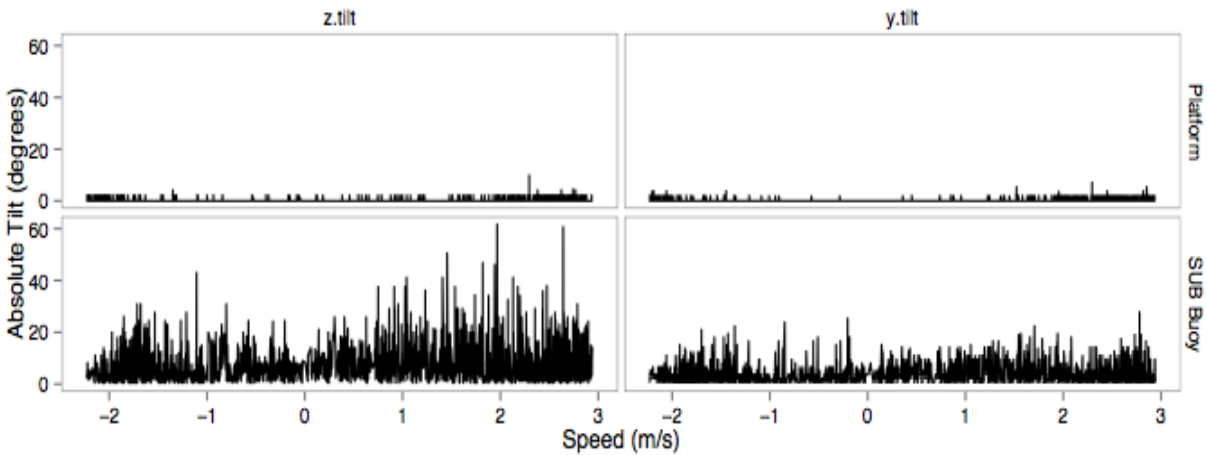


Figure 4.5. Tilt plots for the instrument platform and a SUB buoy co-located at station location W1. Plots compare pitch (*z.tilt*) and roll (*y.tilt*) with depth-averaged current speed (m/s) on the ebb (-) and flood (+) tides.

### **C-POD and icListenHF Range Tests – Platform**

The instrument platform provided a stable platform for the testing of detection ranges for co-located C-PODs and icListenHF hydrophones. An Ocean Sonics speaker, the icTalk, was drifted multiple times over the instrument platform following platform deployments on 2 June 2014 and 12 June 2014 (Figure 4.6). The drift unit consisted of a spar buoy (floatation), rubber tubing (isolates surface movement of floatation from the icTalk), GPS (accurate tracking storing one point every 5 seconds), and chimney sweep brushes to ensure the unit was vertical throughout the water column (Figure 4.7). A metal plate was added to the spar buoy to allow radar to locate the drift buoy.

The icTalk was setup to produce a sound sweep from 120 to 140 kHz, over 0.1s followed by 1s of rest at 140 dB re 1 $\mu$ Pa, and repeated for all drifts. The drifts spanned a 1 km radius from the platform station. icTalk transmissions detected by the icListenHF and C-PODs were examined via visual inspection of the icListenHF spectrograms and C-POD data files.

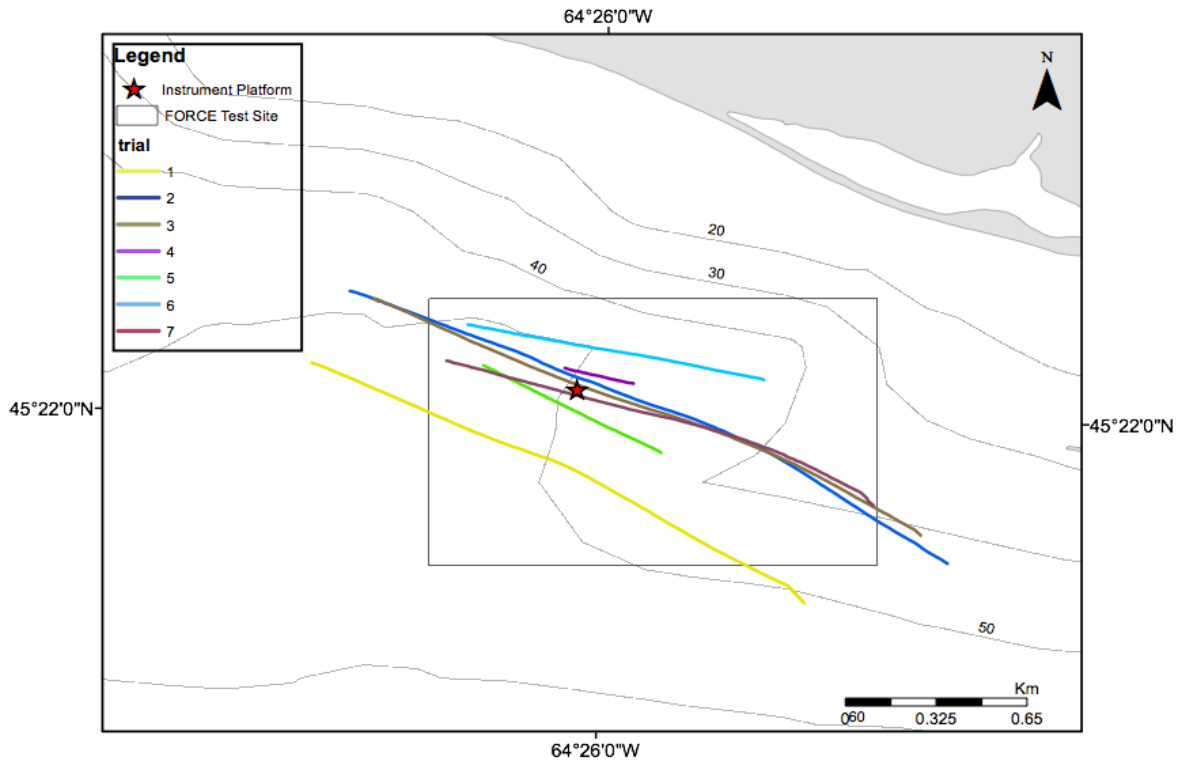


Figure 4.6. *icTalk* speaker tracks through the FORCE site and over the instrument platform that housed two *icListenHF* and two C-PODs (red star, site W1). Most tracks were conducted on the flood tide.



Figure 4.7. Spar buoy with GPS and radar deflector drifting over the instrument platform (lander). *IcTalk* speaker unit is drifting 2 m below the surface.

The detection ranges (bins of 50 m) for the platform housed C-POD 1615 and icListenHF 1239, in relation to depth-averaged current speed, are shown in Figure 4.8. icTalk transmissions detected by the icListenHF were determined manually by visually inspecting the one minute spectrograms. Given that the C-POD does not record raw data but rather provides the user with pre-processed data (CP1 files), any human inspection of the C-POD files is not directly comparable with icListenHF FFT files. The C-POD detected and classified icTalk transmissions at all distances (up 300 m), with most detections at low current speeds ( $\leq 1$  m/s). The icListenHF hydrophone showed detection efficiency or “recall” (fraction of transmissions detected) in the range of 50-100% within 150 m of the icTalk speaker, at all current speeds. Visual inspection of the icListenHF FFT files also showed that 30% of the icTalk transmissions were detected over a distance of 250-300 m, at both low and high depth-averaged current speeds.

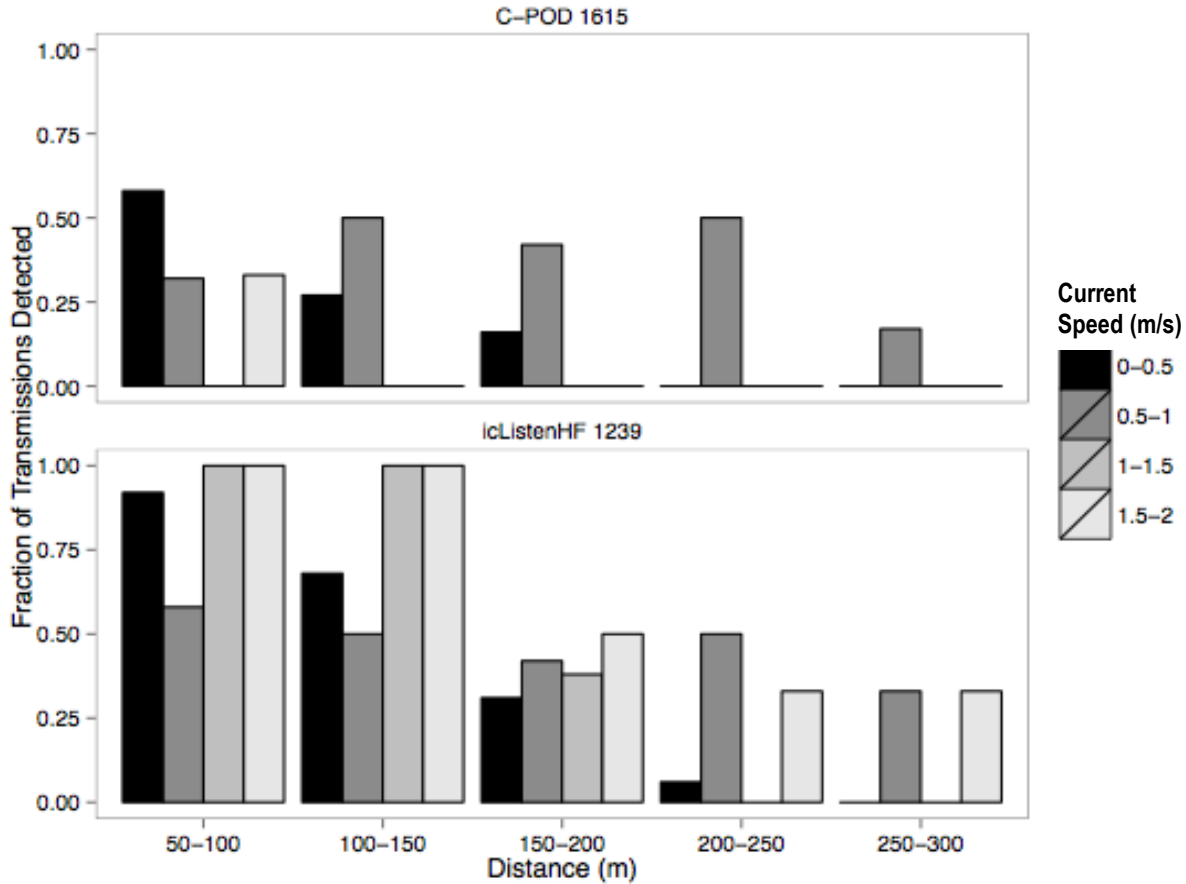


Figure 4.8. Fraction of icTalk transmissions detected by C-POD 1615 and icListenHF 1239 (shrouded) hydrophones. Detections are shown in relation to both distance from the icTalk speaker (drifting in surface waters about 50 m above the bottom) and depth-averaged current speed (m/s). Range test data were collected on 2 June and 12 June 2014.

**Effect of Shrouding on icListenHF Performance – Platform**

Two icListenHF hydrophones, one with and one without a shroud, recorded soundscape data at location W1 (platform mounted) in June 2014. Figure 4.9 shows the mean ambient noise measures (dB re  $1\mu\text{Pa}^2/\text{Hz}$ ) for 120-140 kHz during 6-11 June 2014. The shroud reduced the ambient noise by <3 dB and the highest reduction occurred during high flows on the flood tide (Figure 4.10). Overall, the effect of the shroud at these frequencies was minor.

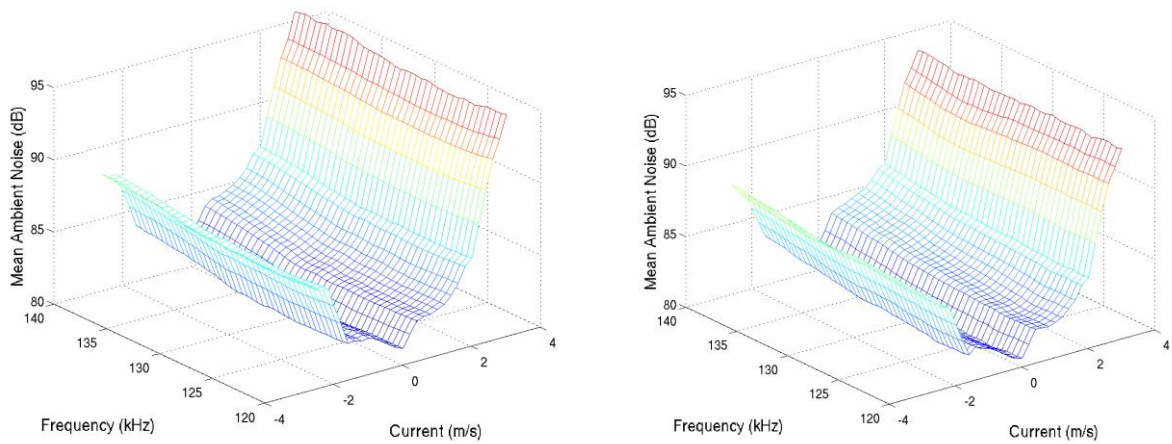


Figure 4.9. *icListenHF* hydrophone measures of mean ambient noise (dB re  $1\mu\text{Pa}^2/\text{Hz}$ ) at 120-140 kHz, as a function of depth-averaged current speed (m/s), at location W1 during 6 June - 11 June 2014. **Left:** hydrophone 1211 without a foam shroud; **Right:** hydrophone 1239 with 0.5 inch, 20 ppi foam shroud.

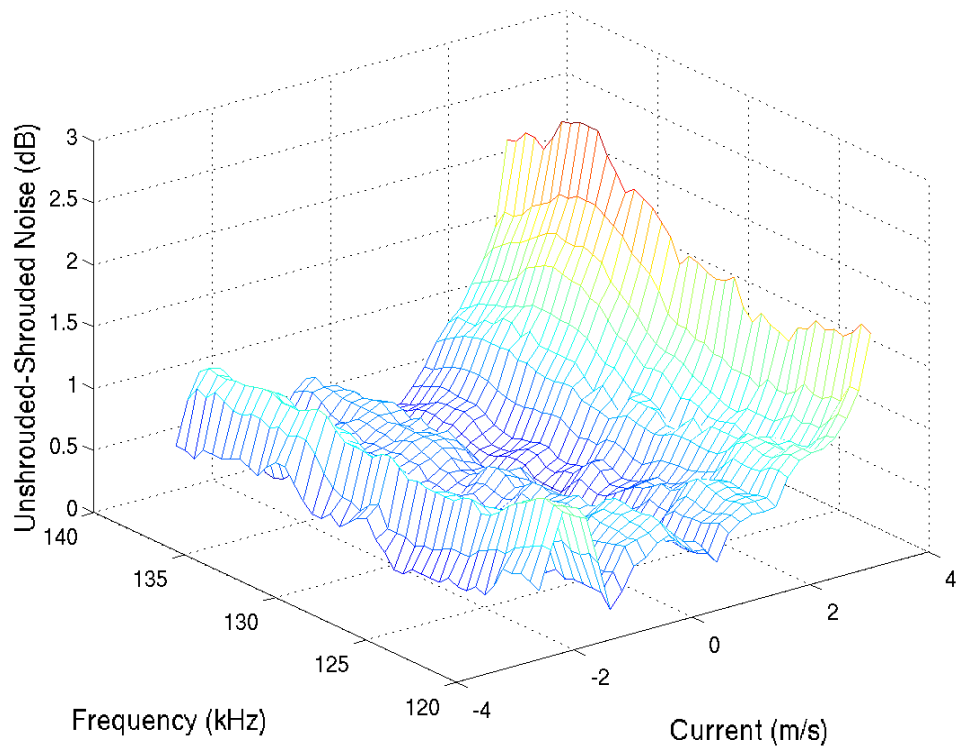


Figure 4.10. The difference in mean ambient noise (dB) between shrouded and nonshrouded *icListenHF* hydrophones in Figure 4.9. Note that the difference is low overall (mostly  $<1$  dB) and greatest at depth-averaged current speeds  $>3$  m/s on the flood tide.

## 5.0 General Discussion and Recommendations

C-POD data collected at several monitoring sites from 4 December 2014 to 2 July 2015 confirm year-round presence of harbour porpoise and was sufficient to close the winter / spring database gap (see Section 2). The updated GAM/GEE model uses the full dataset (2010-2014) to better predict porpoise presence in and around the FORCE test site (Figure 2.3) and identifies those covariates influencing C-POD detection of porpoises. As expected, the new model shows peaks in porpoise activity in late spring (June) and fall (October) with low presence in both summer and winter. The late spring peak in porpoise activity mirrors known movements of Atlantic herring (and other fishes) through the Minas Passage and their capture in intertidal weirs in Minas Basin. Greater porpoise click train detection at night shows that harbour porpoises could be using this time to feed. As shown in Wood et al (2013), porpoises tend to avoid shallow water, preferring depths of 50 m or greater. This extended dataset and statistical model now provides the baseline information needed for turbine installation/operation effects monitoring at FORCE, and will inform the development of the environmental effects monitoring program.

Shrouding of the icListenHF hydrophone tip was tested as a means to improve porpoise detection while limiting % time lost during high flow speeds. Shrouding with acoustic foam (20 ppi, 0.5 inch) was shown to reduce flow noise in the tank tests. But in the field, the shrouded hydrophone recorded a similar sound profile to the non-shrouded unit for the target frequency range 120-140 kHz (difference was < 3dB), with the difference being greatest at high current speeds on the flood tide (Figure 4.10).

An icTalk speaker was used as a sound source to mimic captive harbour porpoises for range testing purposes. Wild harbour porpoises can generate sounds 40 dB greater than captive porpoises (Vil-ladsgaard *et al.*, 2007) so the actual detection range for harbour porpoises in Minas Passage is likely to be higher than that determined with the icTalk drift test. Regardless, both hydrophones recorded icTalk transmissions at up to 300 m, with detection efficiency (“recall”) being greatest at distances <150 m. As with prior studies in Minas Passage (Tollit et al 2011, Wood et al, 2013), C-POD detections at high current speeds (i.e. high ambient noise) were limited.

The two mooring types examined (tethered SUB buoy and bottom platform) presented different environmental conditions for hydrophone performance, and these are reflected in % time lost in C-POD recordings (Figure 4.4) and in tilt sensor data (Figure 4.5). Both % time lost and tilt were lower for C-PODs housed in the bottom-moored platform. The tethered SUB buoy (2-3 m above bottom) experiences extreme changes in tilt (up to 60 degrees) at high flow speeds compared to the platform, which remained in place throughout the deployment period. Noise that is generated by shackle and chain moment, vibrations, and strumming are likely to increase C-POD % lost time. C-POD comparisons at the same site (W1) showed that a platform mounted C-POD detected more harbour porpoise click trains than a C-POD housed in a SUB buoy unit (Figure 4.3).

Spatial and temporal environmental monitoring requirements will likely dictate what hydrophone type or types are deployed. Given the cost of hydrophone deployments (hydrophone unit and batteries, mooring infrastructure, charter costs for field deployment/retrieval) and associated costs in data processing, future harbour porpoise monitoring efforts at FORCE should consider a combination of detection methods - use of an instrument platform (preferably cabled), with both C-PODs and a hydrophone, at one (or more) key sites within the FORCE Crown Lease Area, supplemented with multiple lower cost tethered SUB buoy units (housing C-PODs), deployed at pre-established monitoring sites (Wood *et al.*, 2013). This combination of approaches would provide sufficient temporal and spatial coverage in detecting harbour porpoises when collecting environmental effects monitoring data for comparison with baseline trends.

Based on this and other marine mammal studies conducted to date in Minas Passage, it is recommended that plans for environmental effects monitoring of harbour porpoise at the FORCE test site, following deployment and operation of TISEC devices, consider the following comments and suggestions.

1. At a minimum, two four-month periods of harbour porpoise monitoring per year. One deployment should start in early April and the other in early September to record both the spring and fall peaks in harbour porpoise presence. Given that few harbour porpoises are present year round, it may not be cost effective to monitor all monitoring sites throughout the year.
2. Considering the limited detection range of C-PODs, the likelihood of hydrophone failure (e.g. battery disconnect), and “lost time” associated with excessive noise during high flows, multiple C-PODs should be deployed at each of the previously established monitoring sites (W1, W2, S1, S2, and E1) to increase the chances of detecting harbour porpoise clicks. C-PODs should be deployed in SUB buoys so that direct comparisons can be made with the baseline trends (2010-2013). If possible C-PODs should also be deployed along the southern shore of Minas Passage to better understand passage-wide harbour porpoise presence.
3. Future studies at the FORCE test site should include at least one hydrophone with a click identifier running in real time. The hydrophone should be moored on a cabled, stationary instrument platform along with at least two C-PODs. A bottom-moored, cabled hydrophone would serve to validate C-POD harbour porpoise detections.
4. FORCE is currently testing a recently developed cabled sensor platform in the FORCE Crown Lease Area. This platform could be used to pair hydrophones with other sensor technologies. These could include sonar imaging systems, which can verify hydrophone detections of harbour porpoises and also detect other marine life.



## 6.0 References

- Chelonia Lt. 2013. [http://www.chelonia.co.uk/C-POD\\_standardisation.htm](http://www.chelonia.co.uk/C-POD_standardisation.htm). **Access date:** 14 Nov 2013.
- DFO. 2012. Appropriateness of Existing Monitoring Studies for the Fundy Tidal Energy Project and Considerations for Monitoring Commercial Scale Scenarios. DFO Can. Sci. Advis. Sec. Sci. Resp. 2012/013.
- FORCE 2012. Annual Report 2012. Halifax. 25 pp. (<http://fundyforce.ca/media-center/reports-and-presentations/>)
- Fox, F., and Weisberg, S. 2011. An {R} Companion to Applied Regression, Second Edition. Thousand Oaks CA: Sage. URL: <http://socserv.socsci.mcmaster.ca/jfox/Books/Companion>
- Genz, A., Bretz, F., Miwa, T., Mi, X., Leisch, F., Scheipl, F., and Hothorn., T. 2014. mvtnorm: Multivariate Normal and t Distributions. R package version 1.0-2. URL <http://CRAN.R-project.org/package=mvtnorm>
- Goodson, A.D., and Sturtivant, C.R.1996. Sonar characteristics of the harbour porpoise: source levels and spectrum. ICES Journal of Marine Science 53: 465-472.
- Højsgaard, S., Halekoh, U., and Yan, J. 2006. The R Package geepack for Generalized Estimating Equations Journal of Statistical Software, 15:2 1–11
- Kastelein, R.A., Au, W.W., and de Haan, D. 2002. Audiogram of a harbour porpoises (*Phocoena phocoena*) measured with narrow-band frequency-modulated signals. J. Acoust. Soc. Am. 112:1 334-344.
- Langhamer, O., Haikonen, K., and Sundberg, J. 2010. Wave power - Sustainable energy or environmentally costly? A review with special emphasis on linear wave energy converters. Renewable and Sustainable Energy Reviews 14: 1329-1335.
- Ocean Sonics Ltd. 2013. <http://oceansonics.com/ictalk-hf/>. **Access date:** 14 Nov 2013
- OEER 2008. Fundy Tidal Energy Strategic Assessment Final Report. Halifax. 83 pp.
- Porskamp, P. 2013. Passive acoustic detection of harbour porpoises (*Phocoena phocoena*) in the Minas Passage, Nova Scotia, Canada. B.Sc. (Hon) Thesis. Acadia University, Canada.
- Porskamp, P. 2015. Detecting and assessing trends in harbour porpoise (*Phocoena phocoena*) presence in and near the FORCE test site. M.Sc. Thesis, Acadia University, Canada.
- R Core Team. 2014. R: A language and environment for statistical computing. R Foundation for Statistical Computing, Vienna, Austria. URL: <http://www.R-project.org/>.
- Scott-Hayward, L., Oedekoven, C., Mackenzie, M., Walker, C., and Rexstad, E. 2014. MRSea package (version 0.2.0): Statistical Modelling of bird and cetacean distributions in offshore renewables development areas. University of St. Andrews: Contract with Marine Scotland: SB9 (CR/2012/05), URL: <http://creem2.st-and.ac.uk/software.aspx>.
- Stewart, B.S., Clapham, P.J., Powell, J.A., and Reeves, R.R. 2002. The national Audubon society guide to marine mammals of the world. Alfred A. Knopf, New York.
- Tollit, D., Wood, J., Broome, J., and Redden, A. 2011. Detection of marine mammals and effects monitoring at the NSPI (OpenHydro) turbine site in the Minas Passage during 2010. Final Report to the Fundy Ocean Research Center for Energy. 36 pp.
- Urlick, R.J. 1984. Ambient noise in the sea. Naval Sea Systems Command Department of the Navy Washington, D.C.

- Villadsgaard, A., Wahlberg, M., and Tougaard, J. 2006. Echolocation signals of wild harbour porpoises, *Phocoena phocoena*. *J. Exp. Biol.* 210: 56-64.
- Wood, S. 2014. Fast stable restricted maximum likelihood and marginal likelihood estimation of semiparametric generalized linear models. *Journal of the Royal Statistical Society (B)* 73:1 3-36.
- Wood, J., Tollit, D., Redden, A. Porskamp, P., Broome, J., Fogarty, L., Booth, C., and Karsten, R. 2013. Passive acoustic monitoring of cetacean activity patterns and movements in Minas Passage: Pre-turbine baseline conditions (2011-2012). Final Report to the Fundy Ocean Research Center for Energy and the Offshore Energy Research Association of Nova Scotia. 61 pp.

## 7.0 Acknowledgements

This project was funded by the Offshore Energy Research Association (OERA) of Nova Scotia, MiTACS Accelerate in partnership with FORCE and Ocean Sonics Ltd, and an NSERC Engage grant with Ocean Sonics Ltd. Fisheries and Oceans Canada provided the sensor platform and ORE Sport acoustic release. Mike Stokesbury provided access to an icListenHF hydrophone and Mark Wood and Chris Cook of Ocean Sonics Ltd. assisted with shroud selection, flow tests, and provided a battery pack and icTalk smart projector for range testing. Hydrophone calibrations at Ocean Sonics were conducted by David Sampson. The Ocean Tracking Network at Dalhousie University provided acoustic releases for C-POD SUB buoy deployments. Jeremy Broome, Freya Keyser and vessel captains Mark Taylor, Bob Vaughan and their crews assisted with field work. Brian Sanderson provided hydrophone soundscape plots, and modelled tidal height, current speed and velocity data, as determined using Richard Karsten's model of currents in Minas Passage. Connor Sanderson and Mike Adams assisted with visual inspection of icListenHF spectral data and C-POD data, respectively. GAM/GEE modelling assistance from SMRU Consulting - Dom Tollit, Jason Wood, Ruth Joy and Cormac Booth - was greatly appreciated. Helpful guidance was also provided by Hilary Moors-Murphy and Jack Terhune.

## 8.0 Appendix

Table A1. Concordance correlation coefficients (CC) for the significant DPM10M covariates in the original GAM/GEE model with 2011-2013 data (Wood et al. 2013). Based on CC values each covariate was ranked. See related plot below (Figure A1).

Covariate	Full CC	Covariate CC	Difference in CC	Rank
Julian Day	0.1129	0.0820	0.0309	1
Tidal Velocity	0.1129	0.0906	0.0223	2
Tidal Height	0.1129	0.0927	0.0202	3
Location	0.1129	0.0969	0.0160	4
DNI	0.1129	0.0979	0.0150	5
% Time Lost	0.1129	0.0989	0.0140	6
Click Max	0.1129	0.1127	0.0002	7

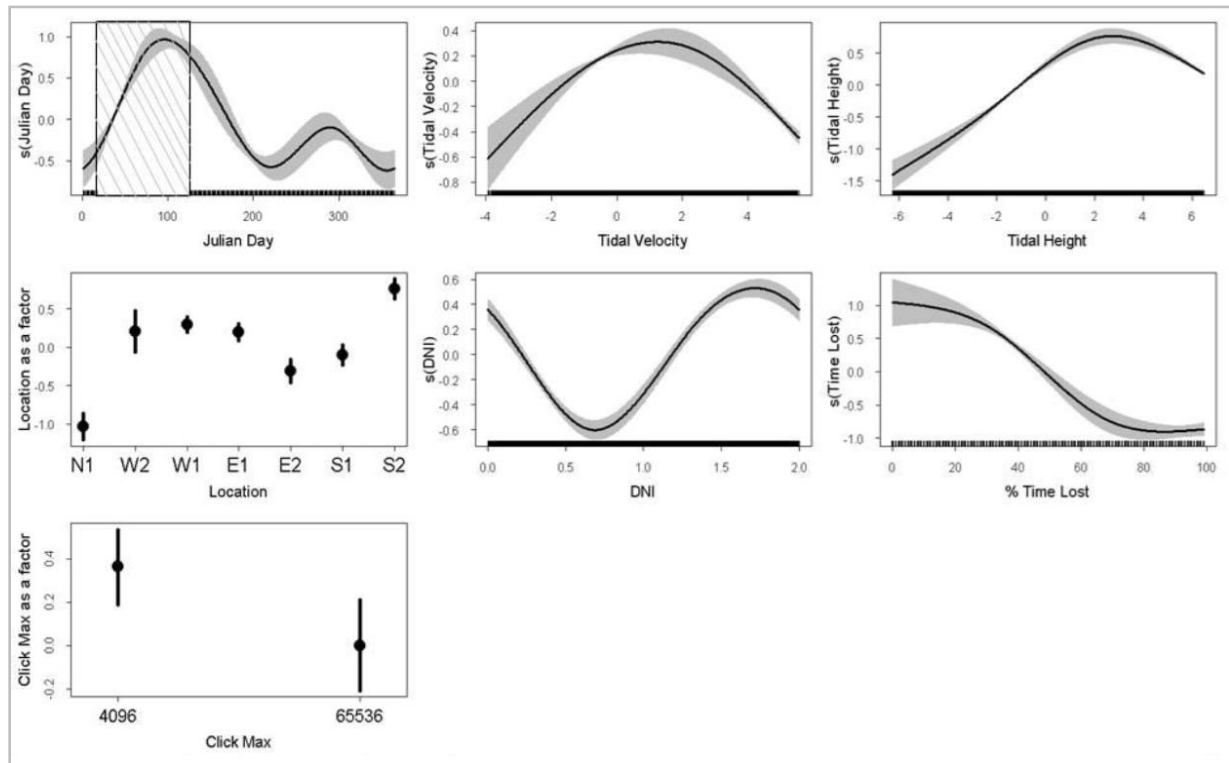


Figure A1. GAM/GEE plots of significant covariates and their relationship to porpoise DPM10M for spring- fall data during 2010-2013 (Wood et al., 2013). Shaded areas and error bars represent 95% confidence intervals. Covariates are shown in order of importance. Diagonal lines in the Julian Day plot indicate a period of no data.